Faculty of Science and Engineering

Department of Chemical Engineering

Dynamic adsorption of cationic surfactants at the alkane/water interface

Abdulsalam Hassan Ahmed Salamah

This thesis is presented for the degree of

Doctor of Philosophy

of

Curtin University

December 2015

Declaration

To the best of my knowledge and belief this thesis contains no material previously published by any other person except where due acknowledgement has been made. This thesis contains no material which has been accepted for the award of any other degree or diploma in any university.

Signature: ……

Date: ……

ACKNOWLEDGEMENTS

I thank almighty Allah for giving me the strength, patience, good health to finish this work.

I would like to express my great thankful to my research supervisor, Dr. Chi Phan for his encouragement, trust and precise advices which are the foundations of this research. The unlimited support and impressive contribution that he has were the driving force for this research and assisted to clear a lot of ambiguity. I also acknowledge Dr. Thanh Vinh Nguyen for his comprehensive work on synthesis and characterization of Gemini surfactant.

I would also to thank my co-supervisors, Prof. Ming Ang and Dr. Gia Pham and Prof. Hongwei Wu as a Chair Person of the Thesis Committee.

I would to thank lab technicians of Chemical Engineering and Chemistry Departments, for their assistance and cooperation throughout experimental work time.

Finally, I like to give my best regards to my friends at Curtin University for and others how have help and support me in different ways during my studies time.

Dedication

This thesis is dedicated to my parents for their loving support.

This thesis is also dedicated to my wife for her “sufferance” and my beloved daughters, Malak, Huda and Mayar for their patience and impressive support during my study period in Western Australia.

Abstract

The interfacial adsorption of surfactants is a dominant factor in numerous applications and industrial systems. The applications arise from their influence on the interfacial properties of air/liquid or liquid/liquid interfaces. The outcomes of various processes essentially depend on interfacial properties, which are in turn determined by surfactants characteristics. These characteristics include dynamic and equilibrium interfacial tension. In spite of the numerous studies, the surfactant adsorption at water/oil interface has not been fully described.

In the literature, the majority of thermodynamic models that employed at oil/water interface were derived from equilibrium tension. The modelling work is this study is fundamentally different. The new model used simple equations to relate interfacial to the bulk concentration. Consequently, the dynamic modelling was applied to obtain adsorption parameters. The dynamic model was fitted simultaneously at two different concentrations. Good fittings were achieved and then applied to predict dynamic tension at other concentrations.

In this study, experimental set up of pendant drop method was employed to experimentally determine the dynamic and equilibrium interfacial tensions. Thus, the adsorption behavior of alkyl trimethyl ammonium bromide was investigated on two alkanes (hexane and decane). Furthermore, the modelling framework is extended to a Gemini surfactant. The Gemini surfactants have particular interest due to advantaged surface activities over the common cationic surfactants. In this regard, the dynamics of symmetric Gemini surfactant (C_{14}-C_3-C_{14}) was studied on decane/water interface.

In the first part of the study, comprehensive attention was devoted to the interaction between oil and surfactants molecules at oil/water interface. In the literature, many studies focused on surfactants adsorption itself only, which can be conducted by the reduction in equilibrium interfacial tension. Such studies often disregard the interactions between surfactants and oil molecules. In other words, these theories assumed the presence of oil molecules does not have any influence on surfactant adsorption. This study attempts to cover the deficiency in the field by modelling the dynamic processes of a common surfactant, CTAB at both hexane and decane

interfaces with water. The results indicated strong interactions between alkane molecules and hydrocarbon tails of surfactant at oil/water interface. From the obtained parameters, new physical insights on alkane and surfactants adsorption addition were proposed. The results open new method to correctly predict the interaction between oil and surfactant molecules as well as the effects of the interactions.

In the second part, the dynamic adsorption of a Gemini surfactant, $C_{14}C_3C_{14}$ was studied. The results indicated the Gemini surfactant has very long adsorption at oil/water interface. The comprehensive modelling indicated a complicated behavior of Gemini surfactant at decane/water interface. Most significantly, the results demonstrated a variable and concentration-dependent interaction between the adsorbed molecules.

Publications

Journals Articles

1. Salamah, A., Phan, C. M. and Pham, H. G. (2015). **Dynamic adsorption of cetyl trimethyl ammonium bromide at decane/water interface.** Colloids and Surfaces A: Physicochemical and Engineering Aspects, 484, 313-317.
2. Iglauer, S., Salamah, A., Sarmadivaleh, M., Liu, K. and Phan, C. (2014). **Contamination of silica surfaces: Impact on water–CO2–quartz and glass contact angle measurements.** International Journal of Greenhouse Gas Control, 22, 325-328.
3. Salamah, A., Phan, C. M., Thanh V. Nguyen and Pham, H. G. (2015). **Dynamic adsorption of a Gemini surfactant at decane/water interface.** Colloids and Surfaces A: Physicochemical and Engineering Aspects **(under preparation)**.

Conference

1. Salamah, A., Phan, C. M. and Pham, H. G. (2014). **Dynamic adsorption of cetyl trimethyl ammonium bromide at Dodecane/water interface**. 6th Pacific Rim Conference on Rheology 2014. Melbourne, Australia, 20-25 July.

Table of Contents

List of Figures

List of Tables

List of symbols

^{1}H NMR	Proton Nuclear magnetic resonance
H DOSY	Diffusion Ordered Spectroscopy
CMC	Critical Micelles Concentration
LC	Langmuir Compressibility
FC	Frumkin Compressibility
FIC	Frumkin Ionic Compressibility
A	The measurement of the non-ideality of mixing in the surface layer
B	An empirical factor for modified of Langmuir-Hinshelwood kinetics
c_b	Surfactant bulk concentration (M)
c_s	Surfactant bulk concentration in the subsurface layer (M)
D	Surfactant diffusion coefficient (m^2/s)
g	Gradient strength
K	Adsorption constant (M^{-1})
k_d	Desorption rate (s^{-1})
k_a	Adsorption rate (m/s)
K_L	Langmuir equilibrium adsorption constants (M^{-1})
K_F	Frumkin equilibrium adsorption constants (M^{-1})
K_H	Henry equilibrium adsorption constant (M^{-1})
R	Universal gas constant (J/K mol)
t	Time (s)

T	Absolute temperature (K)
χ	New adsorption constant (M^{-1})
Γ_{eq}	Equilibrium surface excesses (mol/m^2)
$\Gamma(t)$	Dynamic surface excesses (mol/m^2)
Γ_m	Saturated surface excesses (mol/m^2)
δ	Gradient duration (nm)
δ_γ	Standard deviation in equilibrium surface tension models (mN/m)
τ	Integration variable
γ_{eq}	Equilibrium surface tension (mN/m)
γ_0	Surface tension of pure water (mN/m)
$\gamma(t)$	Dynamic surface tension (mN/m)
γ_m	The meso-equilibrium interfacial tension (mN/m)
γ_{min}	Minimum interfacial tension (mN/m)

1 Introduction

1.1 General overview

The phenomenon of interfacial adsorption between two immiscible fluids is a significant process from both theoretical and application perspectives. Interfacial tension is the force that works between two immiscible liquids and has a parallel force acting on a unit surface area [1]. Commonly, interfacial tension is expressed in mN/m or mJ/m2, but may vary with the application-specified definition [2]. The characteristics of interfacial tension are related to surface-active agents: ‘Surfactants'. This is due to their specific properties of self-assembly (adsorption) to different interfaces, characterized by significant deformation depending on their distinctive structure. This property is essentially based on thermodynamic adsorption and represents a significant role in several practical applications and products like emulsification, wetting, coating, foaming, inhibitor corrosion, and biological industrial purposes [3, 4].

1.2 Introduction to surfactants

Surfactants are defined as chemical compounds which are amphiphilic due to their structure, and consist of a hydrophobic group (surfactant tail) with a slight attraction to water, and a hydrophilic group (surfactant head) with a strong attraction to water as shown in Figure (1-1). Their essential features when changing are responsible for their characteristics at the surface and interface. According to mentioned structure the surfactants basically classified due to the charge of polar head groups. Under this concept the surfactants divided into two main types: non-ionic and ionic surfactants. The non-ionic surfactants with no charge in their head group consider water solubility and that returns to their high polarity such polyol groups. The ionic surfactants with charges in their head groups include the following types:

anionic surfactants with negative charge such carboxylate, sulfate and phosphate. Cationic surfactants which studied in this thesis have positive charges, and common example is quaternary ammonium.

Zwitterionic surfactants which consider crucial factor to biology, consist of negative and positive charge in the head group such as sulfobetaine. Gemini surfactants have two head group and two tails with spacer in between typed into cationic (which studied in this thesis) and ionic depending on head charge.

The reasons behind surfactants deployment return to their exceptional capacity to influence the characters of surface and interface. In addition, surfactants function based on the nature and functional groups position. Hence trivial modifications in molecular structure produce a new module of surfactants require a comprehensive understand to their molecular behavior. This property is employed as a quality criterion in a wide range of industrial fields and has remarkable functional significance. Application of surfactants range from; food processing, cosmetics, paint, pharmaceuticals, agrochemicals, petroleum (Table 1), fuel additives, lubricants, and in photographic films [5].

1.2.1 Basics of surfactant adsorption

Surfactants act at the interface and can be shown by the formation of an aqueous solution of surfactants by dissolving in water. The assembly of surfactant molecules modifies water instruction and increases free energy in the system.

Therefore, the contact between the water molecules and the hydrophobic group will be reduced. The hydrophobic group works by rearranging water structure by breaking and permeating hydrogen bonds simultaneously. According to this phenomena, the hydrophobic groups are oriented to reduce water contact and pushed to the interface with oil, and thereby a reduction in surface tension will occur Figure (1-2).

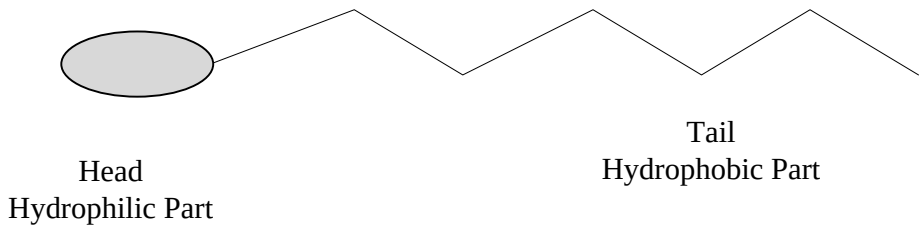

Figure 1-1: Typical structure of Surfactant

In other words, the surfactants' adsorption process is set up in two steps: surfactant molecules transfer from the bulk solution to sub-surface, (the boundary between where diffusion takes place and where adsorption occurs). In the second step, surfactant molecules move to the air interface with the hydrophobic chain pointed out of the water, and hydrophilic head in the water [3, 6]. Therefore, the surfactants reassemble itself at the surface and work on modifying surface characteristics which establish a background for several implementations.

The subsurface concentration is reduced as surfactant molecules adsorb at the interface. As a result, the whole process is dominated by diffusion compared to the amount of adsorbed molecules at the interface layer. The applicable time is the most important part [7] in verifying the diffusion process of surfactant molecules to the interface called dynamic adsorption and extends until equilibrium is established. In other words, the surfactants adsorption continuous (as dynamic) till reach CMC where molecules commence a new state by aggregate and form micellization. After this point the interfacial tension stay constant (no adsorption impact) and does not respond for any increase in the concentration. In case of water is bulk phase the hydrophobic tails intertwined together to reduce water contact whilst the hydrophilic heads stay in contact with water. The formation of surfactants micelles come in different types such bilayers, spherical and cylindrical.

In general, dynamic adsorption is conducted concerning molecule diffusion to the interface [8, 9], and adsorption kinetics are applied when the effective diffusion is too low [10]. On the other hand, the situation become more complicated when air molecules are replaced by oil molecules due to the enriching forces involved in the adsorption layer as shown in Figure (1-3) [11].

However, the surfactant adsorption layer at oil/water interface is important in many practical fields. This area was not highlighted due to the uncertain role of the oil phase. In contrast, a remarkable development has been achieved in the study of adsorption at the air/water interface to determine the kinetics and rheological characteristics from the theoretical and experimental viewpoint.

1.2.2 Measurement techniques

Several difficulties encountered throughout working on the oil/water interface represented in sensitivity of measuring methods to such systems [12], which makes the analysis of the experimental data difficult. Although, most models employed at the air/water interface are directly applied with no specific considerations on the oil/water interface. Limitations in experimental time have some impacts on the experimental process. Potential evaporation of oil, and also purification of all elements participate in the adsorption process.

For instance, surfactant molecules may contain surface contaminations that affect empirical results. This is encountered in the study when cationic surfactants are used as received and take time before commencing purification of surfactants by adopting a crystallization procedure for all used surfactants'.

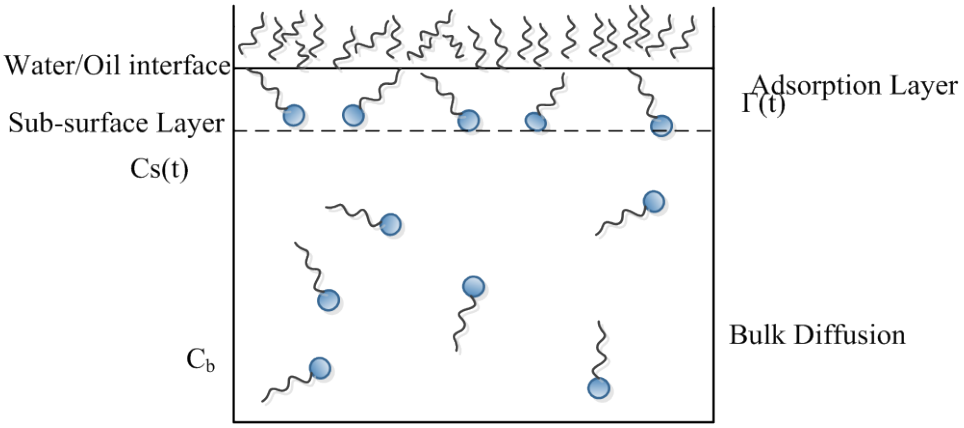

Figure 1-2: Surfactant adsorption process from bulk solution to oil/water interface.

Also, there is a high possibility for surface active molecules to diffuse into oil phase. That requires a purification procedure such as alumina column or silica gel column, the later procedure was applied on different oil phases. Furthermore, the solubility of surfactants in one or two phases complicates the applied conditions and has remarkable effects on experimental outcomes together with the involved partition coefficients [13-15].

There are many methods in the literature that are concerned with measuring interfacial tension between liquids. Each method has its specific considerations that

govern method selection. These characteristics depend on the nature of the measured liquids and the extent of stability. Characteristics also include, experimental circumstances, accuracy, the credibility of applied instruments and the cost [16].

Table 1-1: Some examples of surfactant applications in the petroleum industry [5].

Interface	Applications
Gas/liquid systems	Producing oil well and well-head foams Oil flotation process froth Distillation and fractionation tower foams Fuel oil and jet fuel tank (truck) foams Foam drilling fluid Foam fracturing fluid Foam acidizing fluid Blocking and diverting foams Gas-mobility control foams
Liquid/liquid systems	Emulsion drilling fluids Enhanced oil recovery in situ emulsions Oil sand flotation process slurry Oil sand flotation process froths Well-head emulsions Heavy oil pipeline emulsion Fuel oil emulsions Asphalt emulsion Oil spill emulsions Tanker bilge emulsions
Liquid/solid systems	Reservoir wettability modifiers Reservoir fines stabilizers Tank/vessel sludge dispersants Drilling mud dispersants

The measurement methods include capillary pressure technique, drop profile tensiometer, Du Nouy ring method, Wilhelmy plate method, spinning drop method, pendant drop method, and sessile drop method. It should be mentioned that some methods can only measure equilibrium interfacial tension such as Wilhelmy plate method. On the other hand, some methods, such as the pendant drop method, can be used for both equilibrium and dynamic interfacial tension [17].

The importance of studying the behavior of dynamic interfacial tension is that it offers a deeper understanding of the nature of interactions between different molecules at the adsorption layer. Furthermore, dynamic studies can construct a wider knowledge about molecular arrangements or any effect regarding the aggregation and changes in conformation.

Hence, it can help to understand the basis for chemical reactions and formation kinetics, in addition to the profound illustrations of micellar structure [18].

1.3 Objectives and motivation of the thesis

This thesis aims to study the dynamic and equilibrium adsorption of cationic surfactants: cetyl trimethyl ammonium bromide (CTAB) and Gemini surfactant (C_{14}-C_3-C_{14}) at the alkane/water interface. It aims to develop appropriate models that can be applied to measure dynamic and equilibrium adsorption of surfactants at the oil/water interface. By studying dynamic adsorption, different parameters can be determined such as: adsorption parameters, the nature of interactions between surfactant-surfactant molecules and any roles of oil molecules. It is noteworthy that the work is restricted to below-CMC concentration to highlight the impact of dynamic adsorption [19].

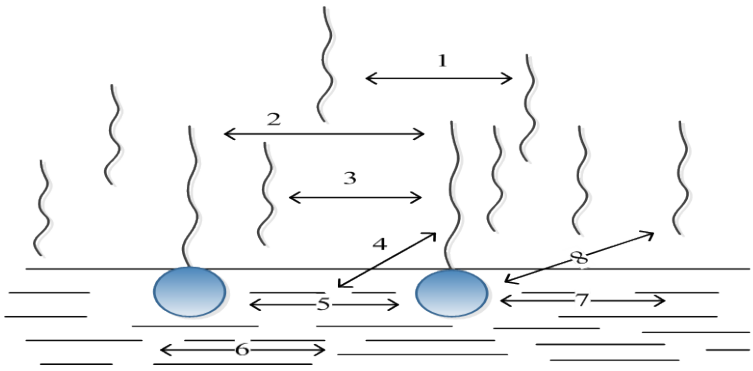

Figure 1-3: Interaction of amphiphiles at oil/water interface; 1- hydrophobic oil/oil, 2- tail/tail, 3- oil/tail, 4- water/oil, 5- head/head, 6- hydrophilic water/water, 7- head/water, 8- head/oil [11].

1.4 Thesis Structure

Chapter 1: Introduce the fundamentals of interfacial tension and its applications in different fields. Provide background about surfactants, fundamental to its adsorption on different surfaces, different methods of measurements and the importance of these measurements in practical life with relation to the significance of this study.

Chapter 2: Presents the theoretical models that are applied on oil/water interface, highlighting the dynamic and equilibrium adsorption behavior. The research gap in this study is to present the relations between different elements that contribute to the reduction in interfacial tension.

Chapter 3: Describe the materials, apparatus, and the instruments that are used to measure the dynamic and equilibrium tensions. The oil and surfactants are purified by the application of silica gel column and recrystallization. Preparation of solutions and apparatus to conduct measurements is also described. These include the experimental data analyzed using axisymmetric drop shape analysis and modelling experimental data by the Excel solver procedure.

Chapter 4: The adsorption behavior of conventional cationic surfactant (CTAB) at different oil surfaces and fitting data determine regarding novel model. This is a comparative study based on a new vision and systematic understanding of the nature of the adsorption process at the oil/water interface.

Chapter 5: Presentation of the Gemini surfactant C_{14}-C_3-C_{14}. Synthesis and measurement of the diffusion coefficient by application of the NMR technique are presented. The chapter also discusses the dynamic adsorption of the Gemini surfactant C_{14}-C_3-C_{14} at the oil/water interface. A new mathematical approach that is successful in predicting the dynamic and equilibrium adsorption is described. The fitting exhibits unusual phenomena and follows two different models (high and low concentrations). Explanations are offered regarding adsorption results.

Chapter 6: An overview of the major conclusions of this work is presented along with some suggestions for further work.

2 Literature Review

2.1 Adsorption behaviour of surfactants at oil/water interface

There are many types of surfactants with a variety of chemical structures and physical properties. These surfactants participate in unique physiochemical virtues at the interface due to the adsorption behaviour characteristics, and self-assembling in bulk solutions. Therefore, understanding adsorption and thermodynamics models is a crucial challenge. The basics of surfactants' adsorption at oil/water interface are as discussed earlier in the case of the air/water interface.

In general, hydrocarbons surface tension is in order of 20-30mN/m, and this attributes to weak molecular interactions in polar solvents [20]. However, the surfactants' presence in the oil/water systems can reduce the interracial tension due to the surfactants transferring and occupying the interface until reaching maximum coverage stage (equilibrium). Also, the influence of adsorption and desorption time affects the interface by expanding or compressing [21].

In regards to the potential solubility of surfactants 'totally or partially' in both liquids [12, 13], surfactant molecules are defined as amphiphilic, i.e., a part works as hydrophilic and the other as hydrophobic. In such cases, at oil/water adsorption, high activity at the surface occurs as a result of the molecules' affinity for oil and water phases [22, 23]. This contributes to the concentration of surfactant molecules at the surface and, therefore, causes the reduction of interfacial tension between oil and water.

For surfactants with complex structure, the diffusion theory is not the only mechanism of adsorption for many conditions. The adsorption in such cases returns to the new orientation of adsorbed molecules, changes in the adsorption layer architecture, and re-change in interfacial structure [24].

The influence of surfactant concentrations on minimizing interfacial tension at oil interface is illustrated in the model situation in Fig. 2-1. In the case of very small concentrations (Fig. 2-1a), the curve is almost straight because the surfactants have no effect on interfacial tension. Thus, it returns to molecules adsorbed away from

each other. Increasing the concentration (Figure 2-1b), leads to the packing of the adsorbed molecules at the interface with significant reduction.

The final stage (Figure 2-1c), is where any increase in concentration is directed to form micelles that take many shapes rather than reducing interfacial tension. This concentration defined as a critical micelles concentration (CMC) [25].

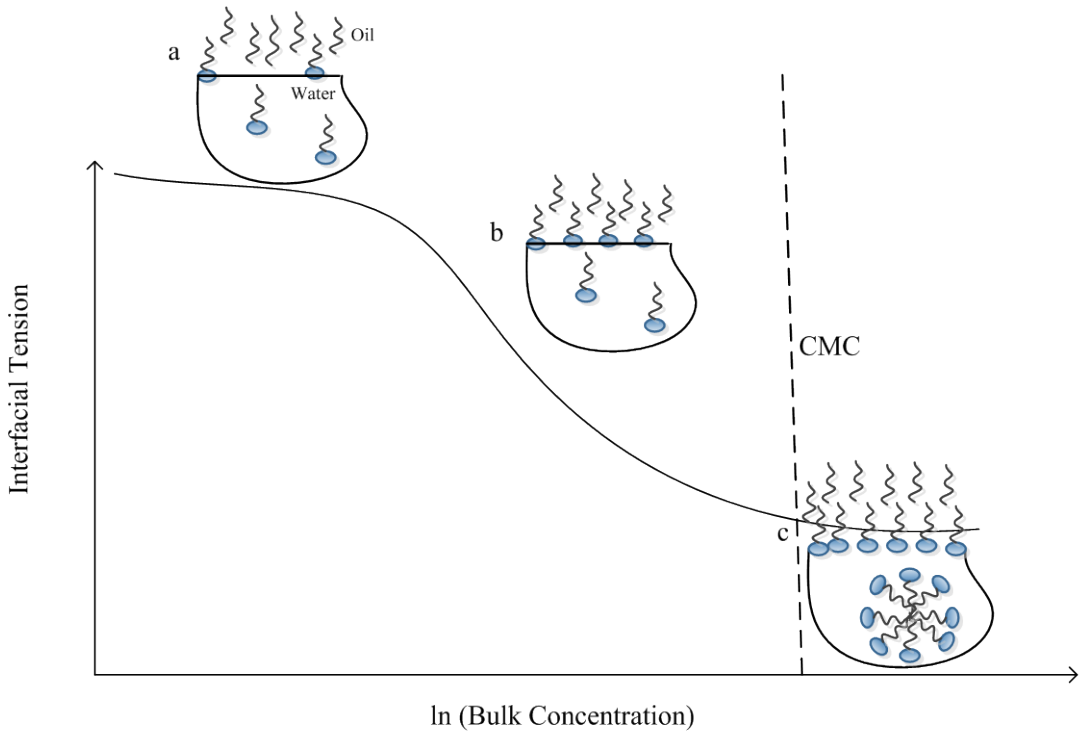

Figure 2-1: Surfactant interfacial concentration as a function of bulk concentration of surfactants on logarithm scale [25].

The CMC is indicated as the clincher point in the plot of surface tension and concentration as the interfacial tension ingredient becomes stable. Micelles formation is considered as another approach mechanism to the adsorption process, where the hydrophobicity of surfactant tails affects the nature of the micelles' orientation.

To reduce contact with water, surfactant tails prefer to agglomerate to each other in bulk solution. This situation contributes to the production of micelles, and in turn arranges itself as oily cores to minimize contact with water molecules [26]. In contrast, surfactant heads (hydrophilic group) remains in direct contact with water

molecules [27]. The emulsions of the surfactant at the oil/water interface take two categories. Firstly, oil in water (O/W) which refers to oil droplet dispersion in water as a continuous phase. Secondly, water in oil (W/O) where the droplet of water (includes surfactant layer) that is dispersed in oil as continuous phase [20].

2.2 Equilibrium interfacial tension

There are a number of methods applied to measure the equilibrium adsorption between two immiscible liquids depending on concepts of single drops or bubbles [11]. Examples of these methods are sessile and pendant drop methods, spinning drop technique and static drop volume method [3, 28, 29]. The experimental data results from these static techniques are compared with theoretical methods to obtain adsorption parameters.

The following section articulates some of the theoretical frameworks that have been used to underpin the analysis of results of this thesis.

2.2.1 Thermodynamic adsorption models

Gibbs adsorption equation is a popular model to calculate the changes in adsorption value of surfactant molecules at the interface and given concentration. This amount of adsorbed molecules is known as adsorption density or the interfacial excess concentration Γ [4]. Interfacial tension measurements can be applied to calculate the number of adsorbed surfactant molecules using the following formula:

$$d\gamma = -\sum_i \Gamma_i d\mu_i \qquad (2\text{-}1)$$

Hence:

dγ change in interfacial tension

Γ_i surface excess concentration of component i

μ_i chemical potential changes of component i

When equilibrium occurs between bulk solution and interfacial phase,

$$d\mu_i = RTd \ln a_i \qquad (2\text{-}2)$$

Where a_i is activity of component i in the bulk, *R* is the ideal gas constant and *T* is the absolute temperature.

For dilute solutions of molar concentration C, the equation can be given in the following form:

$$d\gamma = -nRT\sum_i \Gamma_i d\ln C \qquad (2\text{-}3)$$

At isotherm:

$$\Gamma = \frac{1}{nRT}\left(\frac{d\gamma}{d\ln C}\right) \qquad (2\text{-}4)$$

n is a constant, which refers to the species number between the bulk surfactant and adsorbed surfactant at the interface.

- n=1 for the non-ionic surfactant, or ionic surfactant in excess electrolyte presence.
- n=2 for ionic surfactants without any presence of an excess electrolyte.
- In case of Gemini surfactants, *n* is arguably 2 or 3, or even variable [30].

Adsorption isotherm at equilibrium can be calculated at different bulk concentrations using equation (2-4).

Beside the Gibbs equation, other equations are also used to relate surfactant concentrations at interfacial tension and surfactant equilibrium in the liquid phase. Langmuir model [31], was firstly designed to determine the adsorption at gas/solid surfaces. This model also was valid to measure the adsorption of two immiscible liquids. It is adequately able to describe a variety of experimental results with good agreement.

The fundamentals of the model suggest that each adsorption site is held by only one molecule. Also assumes the ideality in the intermolecular forces, and the interaction between the monomers in the lattice [4].

The corresponding equations of Langmuir model are:

$$\Gamma = \Gamma_m \frac{K_L C_b}{1 + K_L C_b} \qquad (2\text{-}5)$$

or $$C_b = \frac{1}{K_L}\left(\frac{\Gamma}{\Gamma_m - \Gamma}\right).$$

Where c_b is the bulk concentration (mol/l), Γ and Γ_m are the equilibrium and maximum surface concentration respectively (mol/m^2), K_L is the Langmuir equilibrium constant (l/mol).

When $K_L << 1$ at low concentrations at assumption of no interactions between adsorbed molecules, Langmuir isotherm can be described by Henry isotherm [3, 4] as following:

$$k_{H=} \Gamma_m k_L \qquad (2\text{-}6)$$

Here, k_L reverse indicates to surfactant concentrations, where k_H refers to the measurements of surfactants activity.

Szyszkowski equation [32], is another isotherm model derived from substituting Langmuir equation (2-5) to Gibbs equation (2-4);

$$\gamma_0 - \gamma_{eq} = -nR_g T \Gamma_m \ln(1 + KC_b) \qquad (2\text{-}7)$$

Where, γ_0 and γ_{eq} are the interfacial tension of pure solvent and equilibrium interfacial tension respectively. This equation considered as a proof of Langmuir model validity, and provides interpretation for adsorption/desorption mechanism regarding Langmuir adsorption isotherm. On the other hand, Frumkin isotherm [33], considered additional interactions between adsorbed molecules at the interface.

Langmuir model can be replaced by Frumkin isotherm in some conditions, when the model failed to refer to a non-ideal surface. Frumkin isotherm can include the interactions between surfactant molecules at the interface:

$$C_b = \frac{1}{K_F}\left(\frac{\Gamma}{\Gamma_m - \Gamma}\right)\exp\left(-A\frac{\Gamma}{\Gamma_m}\right) \qquad (2\text{-}8)$$

Where K_F is Frumkin equilibrium adsorption isotherm; A is the measure of the non-ideality of mixing in the surface layer.

Eq. (2-8) turned to Langmuir isotherm Eq. (2-5), in case of non-interaction (A=0). The value of A is used to conduct the fitting procedure and my take different signs that have remarkable impacts on interfacial tension (γ) as a function of concentration (Figure. 2-2).

The corresponding equation of state for Frumkin isotherm is:

$$\gamma_0 - \gamma_{eq} = -nR_gT\Gamma_m \ln(1 + \mathrm{KC_b}) - \tfrac{1}{2}nR_gT\Gamma_m \mathrm{A}(\tfrac{\Gamma}{\Gamma_m})^2 \qquad (2\text{-}9)$$

When A has negative sign, this attributes to the attractive interactions between bulk molecules and adsorption layer. Moreover, A may take positive sign and refer to the repulsive interactions between molecules at bulk and adsorption layer [6].

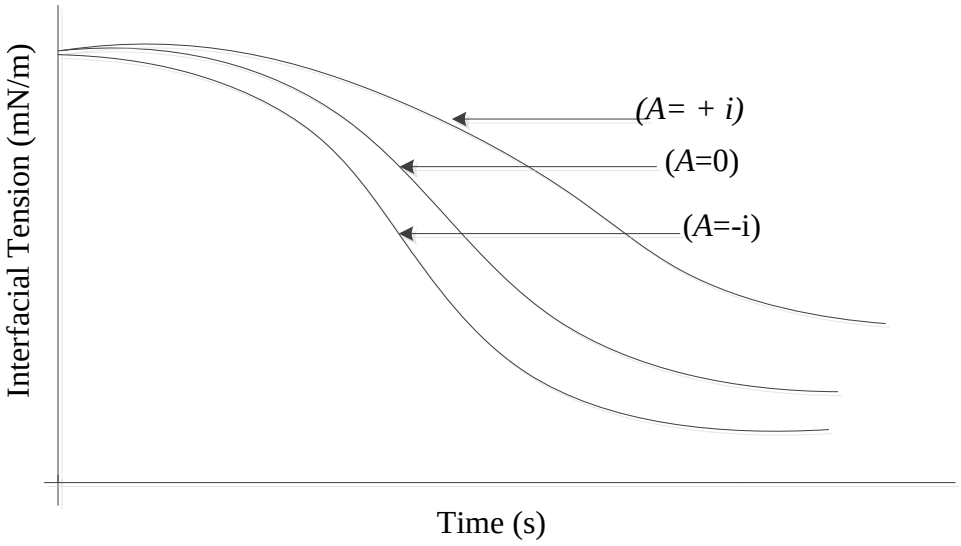

Figure 2-2: The effect of A on dynamic interfacial tension by using Eq. (2-8).

2.2.2 Influences of oil molecules in adsorption layer interactions

The influence of oil molecules in the interactions at the oil/water interface has been the focus of numerous studies. However, there is still an open inquiry concerning the significance of adsorption of both surfactant-surfactant, and surfactant-solvent molecules. Studying the effects of oil molecules on adsorption layer characteristics, with a lot of unverified assumptions, tend to point an insignificant effect of such interactions. This may somehow be attributed to the differences in applied experimental procedures, in addition to use in theoretical frameworks.

A summary of studies that assume the reduction in interfacial tension occurs only by surfactant activity was thoroughly fulfilled and demonstrated by Boucher et al.[34]. After studying the adsorption behaviour of several surfactants, the reduction of interfacial tension at the air/water interface was interpreted under attractive interactions and cohesions between surfactant molecules. However, this is not the case for surfactant adsorption at the oil/water interface, where oil molecules penetrate between surfactant molecules; as a result, the amount of adsorbed surfactant is less than water/air interface.

In similar work, Gurkov et al. [35] studied the stability of interfacial tension of non-ionic surfactants, which have different sizes on the xylene interface. They attribute any decrease in interfacial tension, to surfactant-surfactant adsorption only. Hence, the interactions between oil/surfactants are formed in dipole-dipole interactions excluding ion-dipole interactions.

Danov et al.[36], have measured the adsorption activity of different ionic surfactants at the hexadecane/water interface, and reported that the increase in surfactant concentration leads to gradual increase in surfactant activity Γ_1. The conclusion was based on the notion that the oil molecules are intercalated between surfactant tails. The interactions rates β at the oil/water and the air/water interfaces have been determined by applying different thermodynamic frames such as Van der Waals, Langmuir and Frumkin isotherms. They come to conclude that, the $\beta > 0$ for air/water, and $\beta \approx 0$ at the oil/water interface. This explanation depends on oil molecules that have been squeezed out of adsorption layer. Pradines et al. [13] have also studied the adsorption of a series of alkyl trimethyl ammonium bromides

C_nTAB, at different chain lengths (10,2,14,16) at the water/hexane interface. He pointed out that, for a surfactant with a short alkyl chain, the oil molecules incorporate alongside the surfactant into an adsorption layer. However, the interactions between surfactant molecules exclude oil molecules out of the adsorption layer at longer alkyl chain lengths.

In contrast, there have been many studies that refer to the pivotal role of oil surfactants in adsorption layer structures. That is not only by offering a hydrophobic environment for surfactant alkyl chains to adsorb at the interface, but oil molecules also compete for surfactant molecules to place at the interface. Theoretically, most of the adsorption models to fit experimental data at the oil/water interface have been determined from those developed at air/water interface. Accordingly, this adaptation obviously does not accurately take into account the impact of oil molecules [37]. Medrzycka and Zwierzkowski [38], have investigated the adsorption behaviour of CnTAB (12,14,16) at the air/water interface and the alkane/water interface. In their experiment, they used alkanes that have similar chain lengths as the surfactants. This is to determine the effect of chain length of both molecules on the interactions. They proposed that the oil molecules participate with surfactants depending on the structure of adsorption layer. Fainerman et al. [39] studied the adsorption of a series of alkyl trimethyl ammonium bromides C_nTAB at a variety of water/alkane interfaces. He derived a new thermodynamic model that was originally proposed at different water/alkane interfaces. The interactions in the adsorption layer have been expressed under a mixed adsorption layer. The new theory suggests a competitive case at the interface, between adsorbed surfactant in the solution phase, and alkane molecules in the oil phase.

These consequences has essentially been built on a previous study [40] when the co-author noticed an increase in the adsorption of $C_{10}OE_8$ (octaethyleneglycol monodecyl ether) in hexane-saturated air. The outcomes are interpreted regarding competitive adsorption between $C_{10}OE_8$ and hexane molecules, and imply that the presence of hexane oil contributes to the increase in adsorption of $C_{10}OE_8$. Gillab et al. [41] expected a great increment in the adsorption amount at the oil/water interface against the air/water interface. The adsorption of two ionic surfactants, sodium decyl sulfate (SDS) and sodium dodecyl sulfates (SDDS), have been measured at different

alkane interfaces (C_6–C_{16}). A high adsorption ratio has been found of the aforementioned surfactants at the oil/water interface, with 13 times for SDDS and 35 times for SDS compared to the air/water interface. An earlier study by Hutchinson et al. [42] indicated that the oil molecules are placed at the interface with the adsorbed surfactants. Competitive interactions exist between surfactant alkyl chains and oil molecules. Mucic et al. [15] measured the interfacial tension of two cationic surfactants of series of alkyl trimethyl ammonium bromides (C_{10}TAB and C_{12}TAB) at different alkane interfaces. The affinity of hydrophobic oil chains deduced interface interactions between alkyl chains of surfactant and oil molecules.

It is clear that most studies that avoid any role for oil molecules [13, 34-36] have a good fitting for experimental equilibrium data. However, the good fitting cannot underlie the mechanism of the models. Further, the equilibrium data is insufficient to express the interactions between different energies of the adsorption process at the oil/water interface.

2.2.3 Effect of alkyl chain length of surfactants adsorption

It is crucial to acknowledge the potential impacts of alkyl chain length at the microscopic level on the characteristics of adsorbed surfactants between two immiscible liquids. In this regard, several studies were performed to compare surfactant concentrations' effect on different oil interfaces [23, 43, 44]. Also, oil chain length and its extremity polar appear to have a noteworthy influence on the structure of the surfactant adsorption layer [39]. It can also indicate that the participation of oil molecules in adsorption structure was investigated at water/vapour interface, which considers an intermediate phase between the water/air and the water/oil interfaces. Mucic et al. conducted a comparative study [15], where two alkyl trimethyl ammonium bromides C_{10}TAB and C_{12}TAB were investigated on different aliphatic alkane/water interfaces. As ionic surfactants, the solubility of oil and surfactants was neglected rather than surfactant transfer to the oil phase. It was reported that the value of constant adsorption K and the maximum adsorption Γ_m are much higher compared to air/water interface.

The results qualitatively indicated the intercalation of oil molecules in the adsorption layer of surfactants. The behaviour of both surfactants regarding adsorption parameter values is significant, and yet there is no clear dependence of these parameters on the length of oil molecules and surfactants. This can be potentially interpreted as the specific effect of oil molecules on the surface activity of surfactants. However, Fainerman in his review [45] attributes that to the influence of experimental error. Pradines et al. [13] studied the influence of alkyl chains on fixed oil interfaces. He reported about oil molecules' involvement in adsorption layer with surfactants at the shortest alkyl chain length (C_{10}TAB). He attributes that to the fact that hexane molecules are not long enough to construct the adsorption layer with long hydrophobic chains. While at longer chains (C_{12}TAB, C_{14}TAB, C_{16}TAB), oil molecules are not part of the layer structure due to the strong interactions between the alkyl chains of surfactants.

Medrzycka and Zwierzykowski [38] have also studied the influence of chain length by matching between oil molecules' length (dodecane, tetradecane, and hexadecane), and surfactant alkyl chain length C_nTAB (n = 2,14,16). They aimed to determine under what conditions can the length of oil molecules incorporate in surfactant adsorption layer. They indicate a strong dispersive force between surfactant and oil molecules.

Fainerman et al. [45] in his review indicated another opinion on alkane adsorption at adsorption layer. They suggest that the surfactant molecules can affect the-adsorption process even at another layer (second). Using the binary model, Fainerman repeated the fitting of experimental data and good agreement is observed between experimental data and theoretical model compared to those obtained by the applied model [13]. He agreed with Rosen [26] and pointed out that the increase in the length of surfactant alkyl chain contributes in increasing the interactions between surfactant-surfactant chains and surfactants-alkane molecules.

On the other side, there is an important thermodynamic factor has significant impact on surface/interfacial tension reduction: the water entropy and enthalpy. Hu et al. [46] conducted several measurements on nonionic, zwitterionics and cationic surfactants and studied the behaviour of surface entropy and surface enthalpy. Surface water molecules are flexible to rotate and transfer and in to this concept

surface entropy is higher than bulk. The study claimed that water surface tension essentially depends on surface entropy measurements which in turn based on surfactants head group. In addition, the study reported that mentioned surfactants provide a reduction in water enthalpy between 50-70%. Whereas the influence of water entropy reaches close to zero and sometimes het lower (negative numbers) for ionic surfactants. The order of surfactants capability to reduce surface water entropy is as following; ionic > zwitterionics > nonionic.

2.2.4 Gemini surfactants

Gemini surfactants are well known by their special structure that consists of two hydrophilic heads and two hydrophobic chains with a spacer at different lengths in between [47-49]. In literature, Gemini surfactants of bis-quaternary ammonium bromide $[C_mH_{2m+1}N(CH_3)_2\text{-}(CH_2)_s\text{-}N(CH_3)_2C_mH_{2m+1}]Br_2$ are common regarding properties and surface activities. These Geminis possess symmetrical structures and are referred to as *m-s-m,* where *m* is the carbon atoms' number in the two tails and *s* is the number of carbon atoms in the spacer [30, 50]. In this thesis, gemini surfactant with structure depicted in Figure 2-3 was synthesized with high purity in the laboratory. The steps of synthesis and reaction conditions are detailed later in chapter 5.

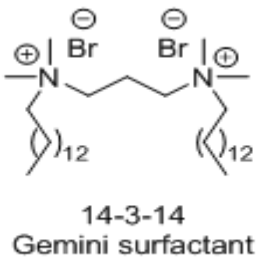

Figure 2-3: The chemical structure of Gemini surfactant $C_{14}\text{-}C_3\text{-}C_{14}$

On the other hand, some Geminis have more than two heads and tails and sometimes different tail lengths and are known as unsymmetrical Geminis [51-55]. In comparison to their conventional surfactants, Gemini surfactants have superior

properties that are influenced by the length of the spacer group, hydrophobic chain length and dissymmetry. Their unique surface active characteristics have attracted considerable interest. One of these features is the observed low critical micelles concentration (CMC). Besides, the viscosity of aqueous Gemini surfactants with a short spacer is much higher than monomeric analogue surfactants at low concentrations and has excellent efficiency in reducing the interfacial tension [30, 56-62]. These properties played an apparent role and introduce better performance in a wide range of applications in different fields such as floatation, food industry, detergents, drug delivery and enhanced oil recovery [63]. In the past few years, a lot of attention have been paid to exploit Gemini surfactants as potential gene delivery agents [64] and the inhibitors of corrosion [65].

Dynamic and equilibrium adsorption of surfactants attracted extensive interest due to their major applications in different industrial and scientific fields. The kinetics of adsorption is almost considered to be an indispensable step to investigate surfactant solutions. This physical phenomenon assists in providing a deep understanding of the behaviour of surfactant molecules throughout the adsorption, in addition to defining the parameters that control the adsorption process [4, 38, 45, 66-68]. Many studies have been conducted on the adsorption of Gemini surfactants at the air/water interface [69-73]. Achyrya et al [58] investigate the dynamic surface tension of gemini surfactants at the air/water interface and claim that the adsorption was very slow in comparison to conventional surfactants and this can be attributed to the complicated molecular structure. Rosen et al [54] investigated the behaviour of dynamic adsorption of two series of cationic Geminis' aqueous solutions and they claim the spacer impacts on the adsorption process.

In contrast, kinetic adsorption of Gemini surfactants at the oil/water interface has not been explored to great details [74-76]. This is partially attributed to the fact that liquid/liquid interface is unstable, thin and buried interface between bulk liquid interfaces. Du et al [74] studied the adsorption of different Geminis at different oil/water interfaces. Experimentally, they measured the dynamic interfacial tension of heptane and tetradecane/water interfaces. All physical quantities were calculated (not fitting) and the influence of the diffusion coefficient hasn't been mentioned. They claim that the increase in alkyl chain length increased the time to reach a stable

value of interfacial tension and this is illustrated regarding the slower diffusion. Using spinning drop method, Zhang et al [77] measured the dynamic interfacial tension of Gemini surfactant against Hexadecane/water interface. Unusual behaviour of surface tension versus concentrations was reported and explained regarding the multi-layer structure. Therefore, promoting procedure to measure dynamic and equilibrium interfacial tension of Geminis is somehow complicated and requires developing a theoretical framework able to describe a full experimental data due to unexpected behaviour of Geminis at adsorption layer.

2.3 The dynamics of adsorption at oil interfaces

It is well known that surface active agents can change the characteristics of different surfaces by adsorption. This phenomenon has been applied to several processes and new industrial technologies considering adsorption influences. These industrial technologies are governed under dynamic terms and developing their efficiency based on the use of interfacial active agents. The formation time of fresh, effective interfaces depends on techniques used and can range from milliseconds to seconds. Dynamic properties of liquid adsorption considerably investigated by determined dynamic interfacial tension.

2.3.1 Empirical model (Rosen approach)

Remarkable effort published in a series of eight manuscripts [66, 68, 70, 78-82], Rosen et al. developed a method to analyse the experimental results of dynamic surface tension at air/water interface. In this study, the concept of Rosen's approach was successfully applied in a similar way to experimental data at the oil/water interface. The curve of dynamic interfacial tension can empirically model using Rosen empirical equation [78]. It demonstrates experimental results in a better way with estimating some physical parameters. Moreover, other physical models can be moderated with the current model regarding the simplicity of the mathematical framework [4].

As shown in Figure (2-2), Rosen divided the curve of dynamic interfacial tension into four regions: (I) induction region (II) rapid fall region (III) meso-equilibrium

region and (IV) equilibrium region. The first three regions can be fitted using the following equation:

$$\gamma_t = \gamma_m + \frac{(\gamma_0 - \gamma_m)}{\left[1+\left(\frac{t}{t^*}\right)^n\right]} \qquad (2\text{-}9)$$

γ_m is the meso-equilibrium interfacial tension, t^* is constant with the same time unit, n is dimensionless constant. It should be noted that least square method (which apply curve fitting procedure) is appropriate technique to determine mentioned fitting parameters [83]. The influences of fitting parameters are depicted in Figures (2-3) to (2-5).

As shown in Figure (2-3), the dynamic interfacial tension curve is fallen into the half of γ_0 - γ_m and verified maximum slope at $t = t^*$ [68]. One can recognise extrusive relation link n and hydrophobicity where at high value rapid gradient occur at second region Figure (2-4). Also, the influence of γ_m is identified in Figure (2-5), where the time does not have any effect on interfacial tension reduction. It takes long time to reach γ_m when the concentration is low. Here, it should mentioned that the fitting of other two parameters occurs at $\gamma_m = \gamma_{eq}$ all in case γ_m cannot be recognised in experimental results.

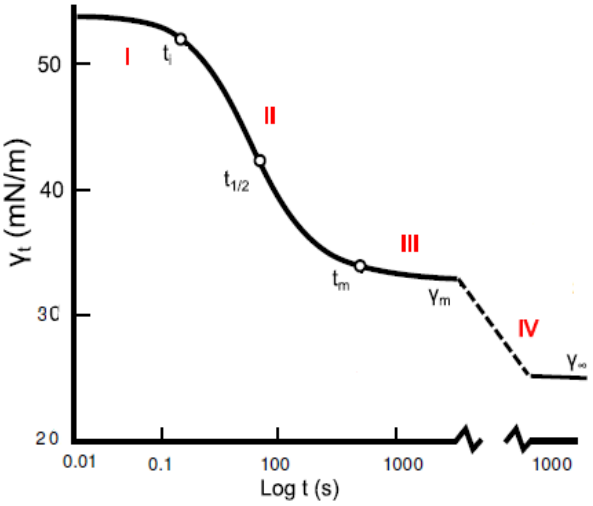

Figure 2-4: Regions of dynamic interfacial tension amended to oil/water interface [78, 84].

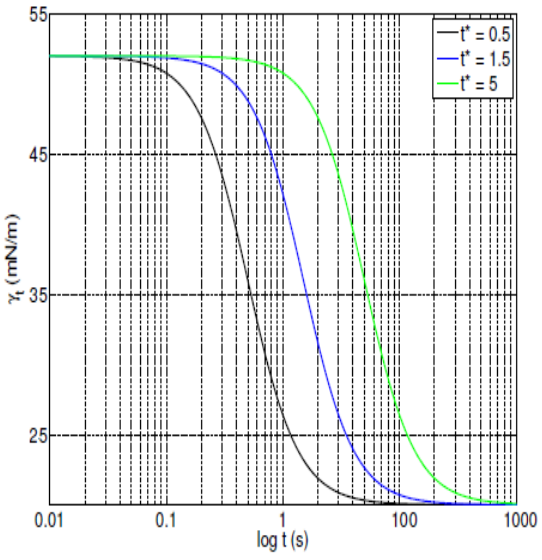

Figure2-5: Rosen approach (t* influence)

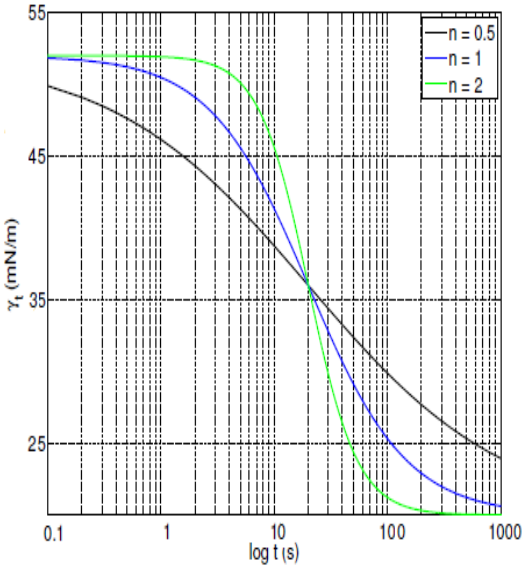

Figure 2-6: Rosen approach (n influence)

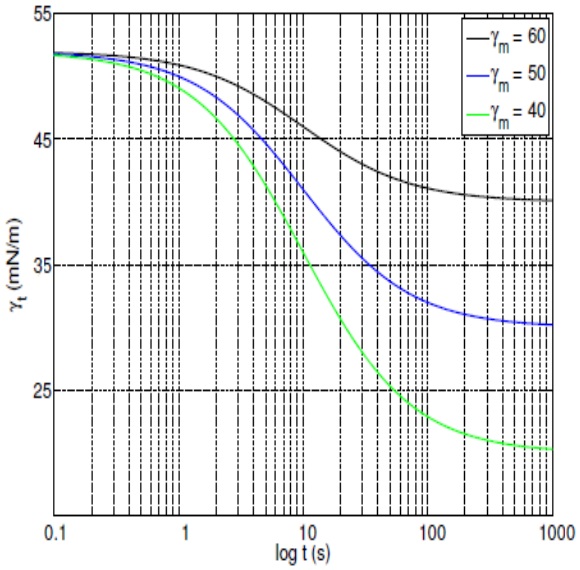

Figure 2-7: Rosen approach (γ_m influence)

2.3.2 Theoretical models for surfactant adsorption

Based on the limitation of interfacial region, and as an instantaneous process. The adsorption concentration determine by Langmuir isotherm that considered in equilibrium with sub-surface concentration [4] as following:

$$c_s(t) = \frac{1}{k}\left(\frac{\Gamma(t)}{\Gamma_m - \Gamma(t)}\right) \qquad (2\text{-}10)$$

Hence, $\Gamma(t)$ and Γ_m represent transient and maximum surface excess concentrations of adsorbed surfactants respectively, $c_s(t)$ sub-surface layer concentration, k is the adsorption constant.

When the system reaches the equilibrium, the concentration of sub-surface and bulk solution becomes similar. As a result, $c_s(\infty)=c_b$ and Eq. (2-10) becomes:

$$c_b = \frac{1}{k}\left(\frac{\Gamma_{eq}}{\Gamma_m - \Gamma_{eq}}\right) \qquad (2\text{-}11)$$

Here, c_b is the bulk concentration, and Γ_{eq} is the equilibrium surface excess concentration.

This procedure also can be applied on Frumkin equation, and reads as:

$$c_s(t) = \frac{1}{k\Gamma_m - \Gamma(t)} \Gamma(t) exp\left\{-A\left[\frac{\Gamma(t)}{\Gamma_m}\right]\right\} \qquad (2\text{-}12)$$

By integration Eq. (2-4), and Eq. (2-10) to form:

$$\gamma_0 - \gamma(t) = -nR_g T \Gamma_m \ln\left(1 + \mathrm{Kc_s(t)}\right) \qquad (2\text{-}13)$$

γ(t) is the dynamic interfacial tension.

The basics of Gibbs equation depend on dividing the surface into several parts. This definition of somewhat is valid in the case of equilibrium interfacial tension. It should be noted that, however, there is no confirmation that the dividing surface maintains its characteristics during dynamic adsorption [85].

2.3.3 Diffusion mechanism

Several studies [3, 86, 87] presented the initial conditions and governed equations of molecular diffusion. Hence, the surfactants molecular diffusion can be determined by the diffusion equation of Fick's second law:

$$\frac{\partial c(x,t)}{\partial t} = D\frac{\partial^2 c(x,t)}{\partial x^2} \qquad (2\text{-}14)$$

$$D\frac{\partial c(0,t)}{\partial x} = \frac{d\Gamma(t)}{\partial t} \qquad (2\text{-}15)$$

at t=0 the initial conditions become:

$$c(x,0) = c_0 \qquad (2\text{-}16)$$

$$\Gamma(0) = 0 \qquad (2\text{-}17)$$

$$c(\infty,t) = c_0 \qquad (2\text{-}18)$$

c(x,t) is the concentration at surface x and time t, *D* is the diffusivity of bulk solution, and c_0 is initial bulk concentration.

The board line between diffusion region (bulk solution), and adsorption region (the interface) is the sub-surface. Surfactants' adsorption to the interface occurs coincidently with a reduction in the concentration of sub-surface. As a result, diffusion process from the bulk occurs to replenish the shortage in the subsurface. Here, it should be mentioned that the rate of molecular diffusivity to the sub-layer is much bigger than that at the adsorption layer.

Numerical methods can offer solutions for diffusion equations by applying appropriate initial and boundary conditions. Thus, an analytical expression is preferable to extract more profound comprehension of the adsorption process. The integral equation of Ward and Tordai [88], has been used to account for the mechanism of diffusion controlled adsorption:

$$\Gamma(t) = 2\sqrt{D/\pi}\left\{c_b\sqrt{t} - \int_0^{\sqrt{t}} c_s(\tau)d\left(\sqrt{t-\tau}\right)\right\} \qquad (2\text{-}19)$$

Where D is diffusion coefficient, τ is dummy integration variable, c_s is the transient subsurface concentration, t is the time and $\Gamma(t)$ is surface concentration excess. The term between the brackets refers to the back diffusion term, and it is also identical to the convolution integral [89]. This model predicts direct adsorption of subsurface molecules to the interface at early times while in contrast some possible deceleration or might back diffusion to the bulk occur at later times [25].

The use of above equation has some difficulties attributes to the unknown boundary of instantaneous sub-surface concentration. It is crucial to apply the appropriate adsorption isotherm to calculate surface excess concentration and sub-surface concentration. In this study, those limits were estimated simultaneously by solving equations (2-10) and (2-17). Besides, Ward-Tordai equation cannot be solved analytically. Hence, a complicated numerical solution is needed. Many researchers [90-93] have performed a remarkable effort to develop a numerical solution for Ward-Tordai equation. Amongst these numerical models, Phan's numerical solution [93] was used in this study.

2.3.4 Diffusion coefficient

As mentioned earlier, surfactant adsorption rate from the bulk solution to the interface between two immiscible liquids depends on its diffusion coefficient and its concentration. Therefore, the bulk concentration is always higher than the subsurface concentration. Diffusivity *D* can be used to describe the necessary time to reach equilibrium.

There are two types of diffusion coefficients: the first is self-diffusion coefficient or tracer diffusion coefficient that is defined as the diffusional movement in singular liquid, and the other kind is the mutual diffusion coefficient, which studies the rate of diffusion of two components, one into another [94, 95]. It was reported earlier [96] that the self-diffusion is considered as a special case of mutual diffusion. In general, the mutual diffusion coefficient is employed to determine the dynamics of surfactants adsorption at liquids [97]. There are different procedures to measure diffusion coefficient such as Nuclear magnetic resonance NMR [98] and dynamic light scattering method [99].

For dynamic adsorption studies, the surfactant concentrations in water are fairly low. Consequently, self-diffusion is employed.

2.3.5 Kinetic mechanism

The above theoretical model may fail to fit experimental data, when obtained diffusion coefficient is larger than theoretical ones [4]. Thus, applying kinetic equation take into account the delay of time due to surfactant transfer from the bulk into the interface.

$$\frac{d\Gamma(t)}{dt} = [\Gamma(t)]\{k^a c_s(t) - k^d F\} \qquad (2\text{-}33)$$

Where, k^a and k^d are adsorption and desorption constant, F and G are Γ(t) functions. The adsorption in this condition depends on Γ(t) and c_s(t) while the desorption just depends on Γ(t). When t→∞ that means dΓ(t)/dt=0, so the Eq. (2-23) becomes:

$$c_s(t)=F(\Gamma(t)) \qquad (2\text{-}24)$$

At equilibrium, the kinetic equation turns into adsorption isotherm [3] and take the following form:

$$\frac{d\Gamma(t)}{dt} = k^a c_s(t)\left(1 - \frac{\Gamma}{\Gamma_m}\right) - k^d\Gamma \qquad (2\text{-}25)$$

This equation represents linear kinetics, the concentration of sub-surface consider as an essential parameter for linearity of the kinetic model together with the empty spaces at the interface (1- Γ/Γ_m). Adsorption and desorption constants k^a,k^d are supposed to be constant. Where,

$$k^a = \frac{k^d}{k\Gamma_m} \qquad (2\text{-}26)$$

It should be highlighted that Eq. (2-25) is a non-linear equation and thus numerical procedures are required. Subsequently, another empirical equation can be used due to the slow in the adsorption rate is expected as the concentration is increased.

$$\frac{d\Gamma(t)}{dt} = k^a c_s(t)\left(1 - \frac{\Gamma}{\Gamma_m}\right) exp\left(-B\left(\Gamma/\Gamma_m\right)\right) - k^d\Gamma exp\left(-B\left(\Gamma/\Gamma_m\right)\right) \qquad (2\text{-}26)$$

Where B is an empirical factor which is used to measure the adsorption and desorption rate.

Accordingly, the effect of surface coverage (Γ/Γ_m) is expected to be similar. The advantages of Eq. (2-26) are represented in better description for the efficiency of surfactant adsorption at high surface coverage. Also, the barrier of activation energy at the adsorption and desorption rate also can be determined.

However, the variation of empirical parameters such as B and k^a with concentration represent a disadvantage. Also, using one term B for adsorption and desorption rate which effect on equilibrium isotherm.

Eq. (2-25) can be extended on Frumkin isotherm to:

$$\frac{d\Gamma(t)}{dt} = c_s(t)k^a\left\{1 - \frac{\Gamma(t)}{\Gamma_m}\right\} - \frac{1}{k}\frac{\Gamma(t)}{\Gamma_m} exp\left\{-A\frac{\Gamma(t)}{\Gamma_m}\right\} \qquad (2\text{-}27)$$

The kinetic model becomes diffusion model in case $k^a \rightarrow \infty$ [93].

It should be noted that the influence of A is just on the desorption rate. To provide more explanation, the following equation that requires numerical solution can be applied.

$$\frac{dt(t)}{dt} = \frac{k^a}{\Gamma_m} exp\left[\frac{A}{2}\left(\Gamma/\Gamma_m\right)^2\right] \times \left[c_s(t)(\Gamma_m - \Gamma) - \frac{\Gamma}{k} exp\left(-A\left(\Gamma/\Gamma_m\right)\right)\right] \quad (2\text{-}28)$$

2.4 Dynamic modelling

2.4.1 Numerical model

Derivation of the theory to describe the experimental data is not simple due to the need for numerical procedures. Thus, precise results can be obtained depending on solving transport equations and, for example, developing techniques to tackle the partial differential equation considered the complex goal. The numerical model can be built to consider the diffusion and adsorbed surfactants, counterions, and electrolyte [11]. In another previous study [93], the numerical solution has been proposed to solve the governing Equations of (2-19) and (2-25).

By dividing the time into small intervals, $\Delta t_i = t_i - t_{i-1}$, i=1,2,3,….. Eq. (2-19) then can be processed by a trapezoidal rule which leads to:

$$g(t_i) \approx \beta - \alpha c_s(t_i) \qquad (2\text{-}29)$$

The dimensionless parameters are defined in the literature [93].

At diffusion the adsorption parameters (c_s(t) and Γm) can obtained by numerical solution for Eq. (2-29) and (2-5) simultaneously where C(0)=0 and Γ(0)=0. Additional parameter A also can be obtained is case of applying Eq. (2-8).

On the other hand, for kinetic model, the Eq. (2-25) can be used with the following frame:

$$\frac{g(t_i) - g(t_{i-1})}{k_a \Delta t_i} = c_s(t_i)[1 - g(t_i)] - \frac{g(t_i)}{k} exp\left(-Ag(t_i)\right) \quad (2\text{-}30)$$

By applying mentioned initial conditions, the Eqs. (2-29) and (2-30) can be solved simultaneously to determine Γ(t).

The regression of non-linear least-square has been used by applying Microsoft Excel spreadsheet with subroutines that are written in Visual Basic. The simultaneous fitting of two dynamic curves took significantly more time than usual fitting. Consequently, the conventional framework, based on Gibbs isotherm is often applied to one concentration at the time only [7].

2.4.2 Fitting of dynamic interfacial data

The experimental results of dynamic interfacial tension are fitted against theoretical models using the following procedure that has been mentioned in [3]. The adsorption equilibrium data is modeled against Langmuir equation using the best-fitted value to obtain adsorption parameters such: k, Γ_m. Another example is Frumkin equation where the model has three parameters: with A as an additional parameter [4]. t also can be extended to include compressibility, Langmuir Compressibility (LC), Frumkin Compressibility (FC) and Frumkin Ionic Compressibility (FIC) [13].

However, the extension requires more parameters. For instance, the Frumkin ionic compressibility model requires up to 6 independent parameters[7]. Besides, Fainerman et al. [39] proposed a new "binary" model, which included a new term accounting for the competitive adsorption of oil and surfactants molecules. The model has more fitting parameters than the air/water interfacial model. However, the proposed model had the same quality of agreement with experimental data and thus cannot be justified from such data.

Secondly, estimating the diffusion coefficient value and comparing it to to a theoretical value that potentially the two scenarios may apply. If the diffusion coefficient value is close to the theoretical value, then the condition is considered as a diffusion process and mentioned adsorption parameters obtained by solving Eq. (2-10) and Eq. (2-19).

The other option the diffusion value is higher than theoretical value and for this case the condition is considered as kinetic process additional adsorption parameters need to be fitted such as ka, kd, β. These other parameters provide better fittings when more complicated models are applied such as modified Frumkin kinetics and modified Langmuir-Hinshelwood kinetics. In the case of using a kinetic step, suitable

fittings can be estimated, but applying the mentioned model requires more parameters. However, the complexity characterizes solution mechanisms and no physical structure for kinetic parameters.

2.4.3 Efficiency and effectiveness of surfactant adsorption

Surfactant molecules reduce the surface tension under two categories: surfactant efficiency where the reduction in surface tension is determined according to concentration and effectiveness where the maximum performance of surfactants can reduce the surface tension with no consideration for the concentration. A criterion for good efficiency when surfactant concentration gives a reduction in surface tension up to 20 mN/m. Hence, this is considered as a minimum concentration required verifying maximum adsorption at the interface. In particular, some parameters may influence the efficiency such as head groups and a straight alkyl chain. The effectiveness of surfactant adsorption is considered a significant factor to assess some applications such as foaming, emulsification and wetting. That is attributing the measurements of interfacial packing by applying maximum surface tension using the Gibbs equation.

The effectiveness and efficiency of surfactant adsorption are not coincidental where sometimes the experimental data exhibits remarkable reducing in surface tension at low concentration (more efficiency), and in contrast smaller maximum surface concentration (less effective) [26, 27].

2.5 New theoretical model

Recently, a new model has been used successfully to model dynamic adsorption at air/water interfaces [55, 70, 71]. This approach is based on the theoretical framework [85] which requires both dynamic and equilibrium data. The model also has been applied successfully to compare the row data of C_{14}TAB and C_{16}TAB [100], as well as a Gemini surfactants [101] at the air water interface.

2.5.1 Theoretical equation

The equation of the new model comes to replace Eq. (2-7), and based on the following relationship;

$$\gamma_{eq} = \gamma_0 e^{-\chi c_b} \qquad (2\text{-}31)$$

Where, γ_{eq} is the equilibrium interfacial tension, $c_s(t)$ is the transient sub-surface concentration [85], and χ is a new adsorption constant with a similar unit of k, which physically applies to the account surfactant efficiency [6].

The mentioned mathematical approach can also be applied to model the dynamic interfacial tension where the relation can be written in form:

$$\gamma(t) = \gamma_0 e^{-\chi c_s(t)} \qquad (2\text{-}32)$$

In this study, the same approach is applied to dynamic adsorption at the oil/water interface. The Ward and Tordai equation, with full numerical solution [93], is used in combination with new modelling approach. Furthermore, the framework can be validated by dynamic adsorption at more than one concentration.

2.5.2 Fitting procedure of new model

Adsorption parameters were fitted simultaneously to two dynamic curves, i.e., two different concentrations was applied to obtain one unique solution. The fitted parameters are *K* and Γ_m which in turn is used to predict another dynamic curve. These fitted parameters also can be used as initial parameters to find the best-fitted value by applying Eq. (2-7). The best value method does not have a fixed value and depends on the initial value. The steps of fitting procedure can be summarised as following:

- Solving eq. (2-7) and (2-31) to determine *K* and Γ_m.
- Estimate the best value of *D* by applying the diffusion model at dynamic experimental data.
- Compare best value of *D* with theoretical value. For small value diffusion kinetic model will be applied to determine the constants.

Here, it should be noted that eq. (2-7) has some circumstances at fittings can be detailed as following: fitting precise of eq. (2-7) to equilibrium experimental results is skeptical in reference to the verities of K and Γ_m that provide good fitting to equilibrium results. The other concern these fittings are just applicable to Langmuir model. Otherwise, if for example Frumkin model or any other models were applied, more other parameters should be concerned.

In this thesis, The new model eq. (2-31) has been applied alongside with eq. (2-7) and one can number some features of novel model:

- The key advantage of the new model is that it has fewer parameters and provides unique solutions.
- The new model has been applied previously to describe equilibrium and dynamic adsorption on the air/water interface [100], and oil/water (chapter 4) where good prediction for experimental data was obtained.
- Excludes surface excess concentration and relates the interfacial tension to bulk concentration. The equation does not depend on Gibbs isotherm (2-4), or Eq. (2-7).

Furthermore, the new model differs from the conventional approach that depends on the specific thickness of the sub-surface layer. The mathematical relationship is consistently applied for all dynamic adsorptions.

The best-fitted parameters determined by calculating the mean square average deviation of experimental and modelling results that verified with following equation:

$$\delta_\gamma = \sqrt{\frac{\Sigma(\gamma_{exp} - \gamma_{model})^2}{n}} \qquad (2\text{-}33)$$

Hence, δ_γ is the standard deviation, n is measured points. The standard deviations of the prediction were also smaller than 1mM/m and indicated good predictability.

This new modelling approach is the theoretical basis for modelling works in this study.

2.6 Other experimental techniques to study interfacial adsorption

One of the problems faced throughout studying interfacial tension is the determination of the structure and order of molecules at the adsorption layer of the oil/water interface. Moreover, some technical issues may affect the reliability of measurements. For example, lack of the efficiency of applied method due to the presence of oil phase, purification of both phases and volatility of oil phase that has an adverse impact on experiment time [102]. Accordingly, some techniques have been proposed for more robust procedures to tackle and provide a better understanding for the width of the interfacial layer and potential ordering at the interface of oil/water.

2.6.1 X-ray studies

This method is defined as a well-established technique to measure the surface and interface parameters. The concept of this technique is based on determining the differences between electron densities as a function of the depth from the interface.

For the oil/water interface, the incoming X-ray beam penetrates the oil phase (K_{in}), and reaches the interface before reflecting on water phase (k_{scat}). The difference between these rays K_{in} and K_{scat} refers to wave vector transfer Q_z Figure (2-3) [103]. Hence, some of the rays have been absorbed by liquid; the angles (α) have adjusted on the scale of a millidegree.

The adsorption of surfactants at the oil/water interface was studied by this method where the outcomes support that the oil presence has a strong impact on the disorder of molecules at the adsorption layer. In addition, change in the length of oil molecules (hexane to hexadecane) has strong effect on adsorbed surfactants where the monolayer is replaced by multi-layer [44].

In this regard, a comparative study [104] showed the full extent of surfactant molecules at oil/water interface, and thereby the thickness layer is much greater than the air/ water interface. Furthermore, they attributed surfactant thickness to the high fluctuation in the layer. Therefore, abnormal roughnesses are anticipated due to high interaction at the interface between surfactant and oil molecules.

In other studies conducted by X- ray, it is indicated that interfacial fluctuation contributes to form the layer at the interface thicker than bulk solution [105]. Ivanov et al. [67] reported the molecules row parallel to the interface at the same plane. Repulsion occurs between compete molecules, and thereby some of them will attempt to expel away from the adsorption layer.

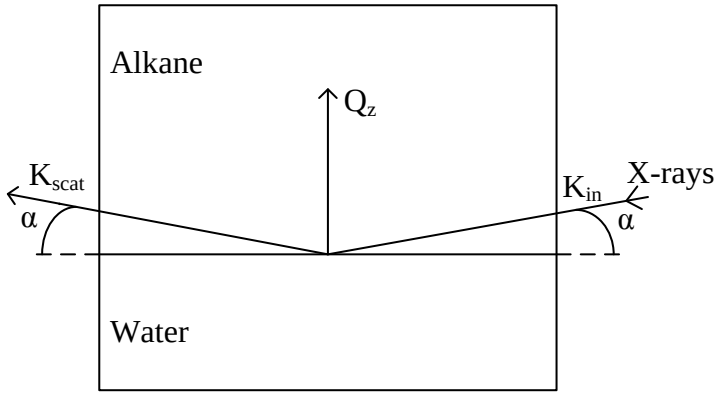

Figure 2-8: X-ray scattering between alkane and water interface [103].

In contrast, the roughness of the interface produces a multilayer adsorption layer. Such position has effects on adsorption energy, where some molecules become deeper into water region than others. This situation reduces the repulsion between molecules and increases adsorption concentration. In the same way, Lu et al. [106] experimentally observed the roughness of layers by applying neutron scattering on different surfactants at the air/water and oil/water interfaces.

Interestingly, they assumed that the surfactant and oil molecules are joining the same roughness. Alongside, surfactant adsorbed molecules are not as vertical as oil molecules and are tilted to enhance layer dimensions and then contribute in the roughness structure.

2.6.2 Neutron reflectometry

This procedure is a powerful technique to investigate the structure of adsorbed surfactants along with impeded interfaces on a molecular scale. The foundation of this method involving concentrated beam of neutrons falls on the planar surface. Neutron reflectometry offers accurate information about the surface structure,

density and also surface roughness. This method is considered as a specular reflection technique where the scattering is elastic and both angles are equal[107]. In particular, neutron reflection on the refractive scale provides much detail about the interface. Thus, the reflective scale is linked to scattering length density of the material and gives the significant information about the composition and orders of molecules at the interface. This information also can be obtained by X-ray, but applying neutron scattering provides a random impact from element to another, and using of isotopic scattering gives clear contrasts in scattering density.

The interaction between the surfactant alkyl chain and hydrophobic oil molecules were investigated by applying neutron reflectometry [104]. Active interactions have been reported which can be attributed to the roughness influence. Accordingly, the interfacial thickness of oil/water is three times thicker than the air/water interface.

2.6.3 Radiotracer

Measuring surface tension using radiotracer technique was firstly developed by Dixon, et al., [108]. However, few types of research have been published in this field due to unexpected problems in determining the radiation emitted on the surface solution by the radio. The principles of this technique are based on verifying the self-adsorption by applying radiation to the solution. Surfactant molecules adsorbed at the interface, and that is a return to the radiation at the interface is stronger than that at the solution. In other the words, this method measures the difference in radioactivity between labelled surfactants at adsorption layer together with solution bulk and at bulk solution alone. Radiotracer was successfully applied to measure the adsorption of sodium dodecyl sulfate solutions SDS, potassium and palmitate. Furthermore, the adsorption of ion from surfactant solution has been investigated using the current technique [109]. Subsequently, the radiotracer is capable of providing interpretations for a mixture of surfactants, the measurements of surface tension may produce data that are difficult to analyse [110]. Nevertheless, the method involved expensive safety equipment due to radioactivity. Hence, the application of radiotracer has been reduced after developing more efficient techniques [11].

2.7 Summary

The fundamentals of different theoretical models and the characteristics of aqueous surfactant solution and their influence on adsorption process on the oil/water interface have been described. In fact, the current understanding of surfactant adsorption at the oil/water interface are not well- detected, and this is attributed to the majority of theories that are applied to the oil/water interface were adopted from models of the air/water interface. The current model relies on equation tension that produces non-unique fitting parameters. Furthermore, the current model failed to describe the impact of oil molecules and surfactant molecules. On the other hand, the experimental data clearly shows the significance of molecular factors on such processes.

Hence, applying dynamic model can provide new methods to overcome such shortcomings. This thesis employs the new methods and aims to produce new insights into the interactions of ions of the oil/water systems. Two systems were selected for this study, and presented in Chapter 4 and 5 respectively.

In Chapter 4, the experimental data for CTAB at both decane/water and hexane/water interfaces, were modelled to obtain the adsorption parameters from dynamic instead of equilibrium interfacial tension. From the adsorption parameters can be used to deduce in influences of alkane on the adsorbed layer.

In Chapter 5, a new mathematical approach has been developed to fit experimental data of the Gemini surfactant. The fitting is applied on dynamic and equilibrium results to determine physical quantities, where some interpretations are produced to illustrate the adsorption at interfacial layers.

3 Methodology

3.1 Chemical and organic compounds

The adsorption behaviour of cationic surfactants (CTAB) and (C_{14}-C_3-C_{14}) were investigated on the oil/water interface. Thus, experimental work was applied to measure dynamic and equilibrium interfacial tensions using the pendant drop method. The experimental data is analysed by computer software and is fitted using different theoretical models.

3.1.1 Hydrocarbons

A series of alkanes (hexane, decane, dodecane and hexadecane) were investigated to determine two essential characteristics:

- The effect of oil molecules on the structure of surfactant adsorption layer.
- Any potential role of oil molecules length on surfactant adsorption behaviour.

The alkanes were undergoing the purification procedure to avoid any contaminated agents that influents alkane surface tension. Table 3-1 elucidates the structure and suppliers of used alkanes.

Table 3-1: Applied alkanes

Alkane	**Formula**	**Supplier**	**Purity**
Hexane	$C_6 H_{14}$	Sigma Aldrich	99%
Decane	$C_{10} H_{22}$	Sigma Aldrich	99%

3.1.2 Surfactants

In this study, two cationic surfactants: (i) cetyl trimethyl ammonium bromide and (ii) α,ω-bis(N-alkyl dimethylammonium bromides) were investigated. There are denoted as CTAB and C_{14}-C_3-C_{14} in this study. The first surfactant is a common cationic surfactant, which was obtained commercially. Subsequently, the surfactant was purified for the study. The second surfactant is a Gemini surfactant, which was

synthesized with high purity. Table 3-2 shows the structures and suppliers of used surfactants.

Table 3-2: Used cationic surfactants

Surfactant	Structure	Supplier	Purity
Cetyltrimethylammonium bromide	$CH_3\ (CH_2)_{15}N\ (Br)\ (CH_3)_3$	Sigma Aldsich	99%
α,ω-bis(N-alkyl dimethylammonium bromides	$[C_{14}H_{29}N(CH_3)_2\text{-}[(CH_2)C_{14}H_{29}N\ (CH_3)_2\text{-}(CH_2)_3\text{-}N(CH_3)_2C_{14}H_{29}]Br_2$	Synthesis	90%

3.2 Purification procedures

One of the parameters that influence the droplet formation is surface active contamination. The effect was experienced in this study where value obtained at equilibrium tensions fluctuated. The effect of impurities typically depends on concentration and can be expressed to resist the transfer of surfactant molecules and may contribute to decreasing internal motion. In spite of the products were provided for a high quality, these products were purified again to avoid any potential effects of contamination.

3.2.1 Alkane purification

In general, the alkanes potentially has traces of surface–active impurities [111]. These impurities have real impacts on the behaviour of interfacial tension at the oil /water interface. Thereby most experiments suffer from a lack of purity and reliability. This was faced earlier in this study when the surface tension of hexane was measured many times resulting in low surface tension at 40 mN/m. The purification procedure is described below.

The glass chromatography column as shown in Figure 3-1 was connected to glass elbow at the top. This elbow is in turn fitted to rubber tube with a manual activation pump at the end. The purified alkanes will be collected from the end of the column in

measured flask. Certain amount of Silica Gel (Sigma Aldrich) placed in a measured flask and well mixed with Petroleum Spirit (Sigma Aldrich). Subsequently, the mixture is placed in the column, and a known amount of hexane will be introduced to the column. Then, the whole amount of hexane will be manually pumped throughout the column. This procedure was repeated several times until the hexane surface tension is verified. The purified dosage fractionated under pressure at a temperature less than melting point of hexane using rotary vacuum. The mid fraction of purified hexane was collected prior to the experiments [112]. A further step is applied where the sample of hexane was tested by NMR (Appendix 2) to guarantee that every trace of petroleum spirit was excluded by comparing with standards. The surface tension of hexane was assessed using pendant drop method and the results were 49.5 mN/m. The effect of purification steps on hexane surface tension is shown in Figure 3-2.

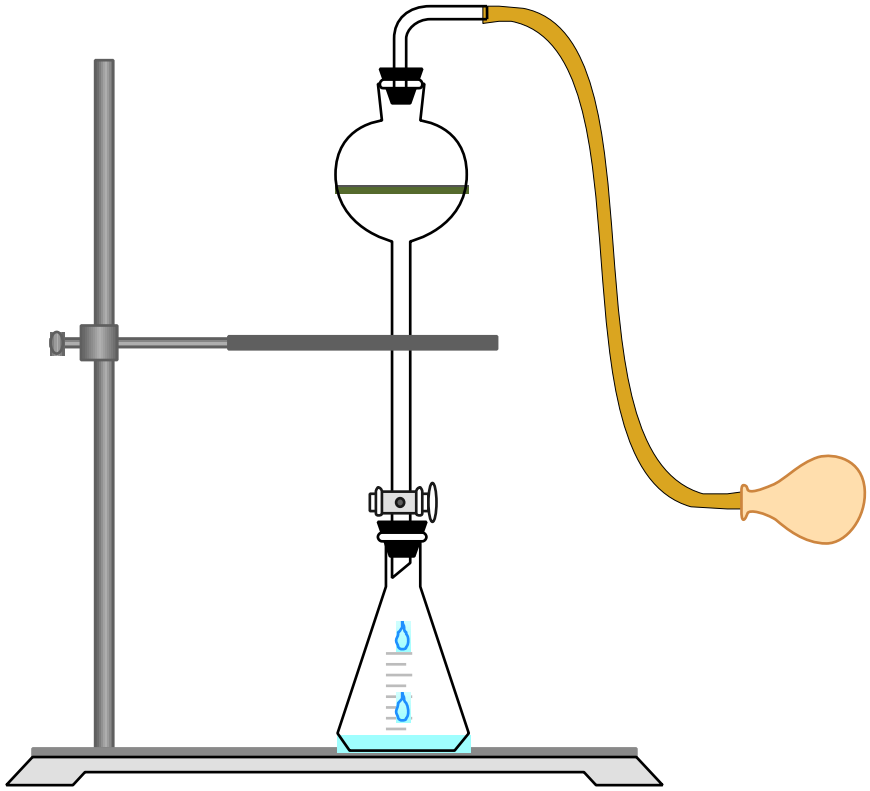

Figure 3-1: Alkanes purification using silica gel column

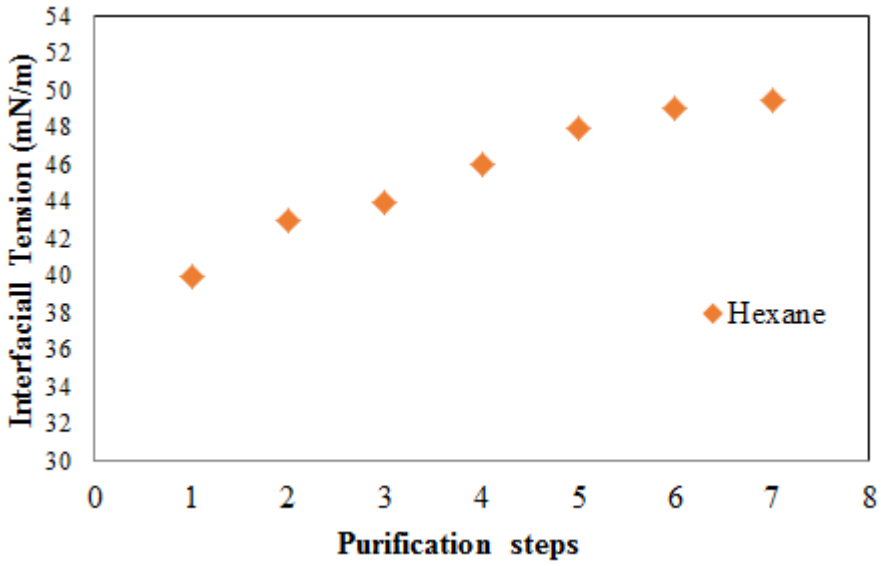

Figure 3-2: Hexane/water interfacial tensions regarding to the step of purification

3.2.2 Surfactants recrystallization

After several experiments at cationic surfactants, it was clear that the impurities have significant impacts on surface characteristics. To evaluate the performance of surfactants, the purification was mandatory.

Recrystallization is a significant method to remove the impurities from the solid component using a solvent. The basics of this method are: increasing the temperature of dissolving the solute close to its boiling point and then cooling to collect crystals.

A. Solvent selection

The appropriate solvent for whole used cationic surfactants was acetone. The process depends on taking a small quantity of surfactant and adding a small quantity acetone until the surfactant cannot dissolve.

B. Recrystallization process

Recrystallization involves:

- In Erlenmeyer flask, put a small quantity of surfactant (5-7 g) and add some acetone (150- 200ml).
- Heat the whole mixture on a hot plate to boiling point.

- Remove the mixture from the hot plate and leave it to be cooled undisturbed at room temperature.
- For a further cooling, place the mixture in the ice bath until the crystals appear.
- Collect the crystals by vacuum filtration and rinse with a small amount of cold acetone.
- Place the purified crystals overnight in the desiccator to verify efficient dryness.
- This procedure is repeated twice and the purified surfactants tested by measuring equilibrium surface tension. Flow sheet of surfactants purification process depicted in Figure 3-3

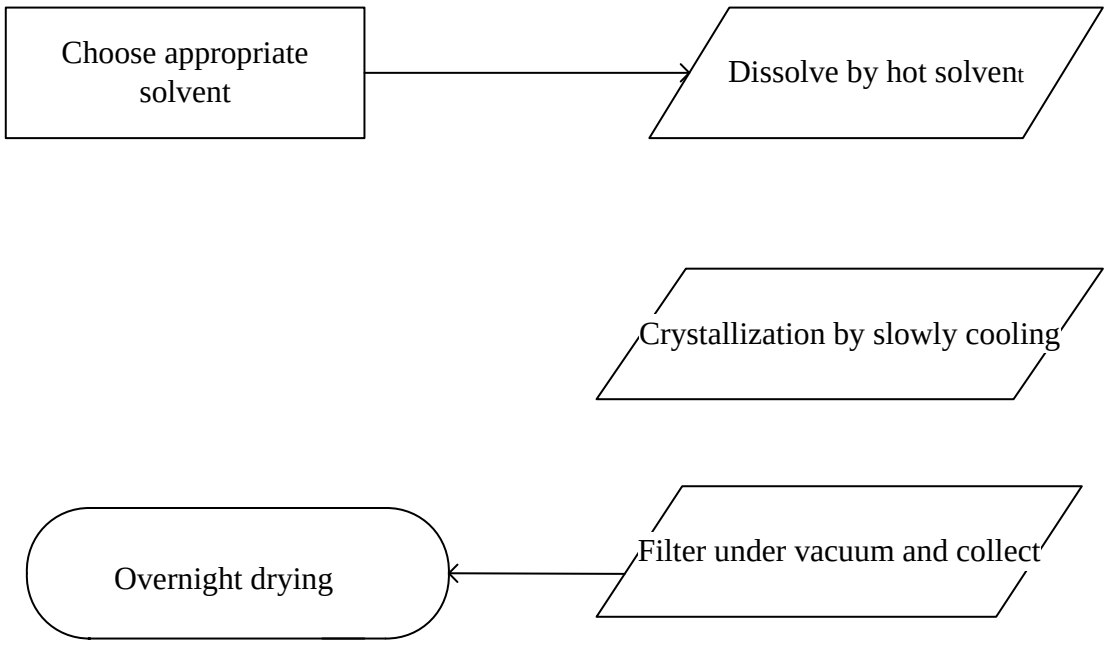

Figure 3-3: Flow sheet of recrystallization process

3.3 Interfacial tension measurements

It is well known that the diffusion of surfactants molecules in liquids is slow. As a result, the measurements of dynamic interfacial tension between two immiscible liquids require a longer time compare to the air/water interface. Regarding these requirements, the measurement options are limited and pendant drop technique is the only appropriate and reliable method.

3.3.1 General principle of pendant drop method

The basics of the pendant drop technique depend on the estimation of interfacial tension from the droplet shape, with minimal interface disturbances. For oil/water measurements, the drop formation will be on the needle tip immersed in liquid. The drop instantly stays hanging which eventually would be detached by gravity. The principle of the surface tension calculation returns to estimate the boundary of drop dimensions related to density criteria. The physical foundation of the pendant drop and calculation method has been mentioned in early studies [113, 114]. There are two methods with the pendant drop.

In the first method, both experimental and theoretical shapes are fitted according to the Laplace equation:

$$\Delta P = \gamma\left(\frac{1}{R1}+\frac{1}{R2}\right) \qquad (3\text{-}1)$$

Where:

γ is the interfacial tension between two phases.

R1, R2 are two principal radii of the drop.

Δp is pressure difference through curved drop.

From fitting the theoretical curve to the raw image of the droplet, the surface or interfacial tension can be obtained [115].

The second method is based on some weight of the droplet, depending on Tate's law:

$$W=2\,\pi\,r\,\gamma \qquad (3\text{-}3)$$

Here, W is the drop weight, r is tip radius.

The first method was chosen due to the flexibility of applying small quantities of liquids. It is also, easily adapted to temperature and pressure. Furthermore, this method allows highly accurate measurements by controlling external vibration. Using this method means only a few drops are required to determine surface tension. Additionally, the experiment procedure is simple and can measure a variety of fluid ranges [116, 117]. With the available fitting software[115], the pendant drop became more convenient for dynamic tension studies.

3.3.2 Experimental Setup

The apparatus of pendant drop as shown in **Figure 3-5** consists of following parts:

- An experimental cuvette covered by metal cap.
- Illuminating system which present a clear vision of the drop,
- Syringe from Hamilton Co. (Nevada, USA),
- Camera,
- Computer.

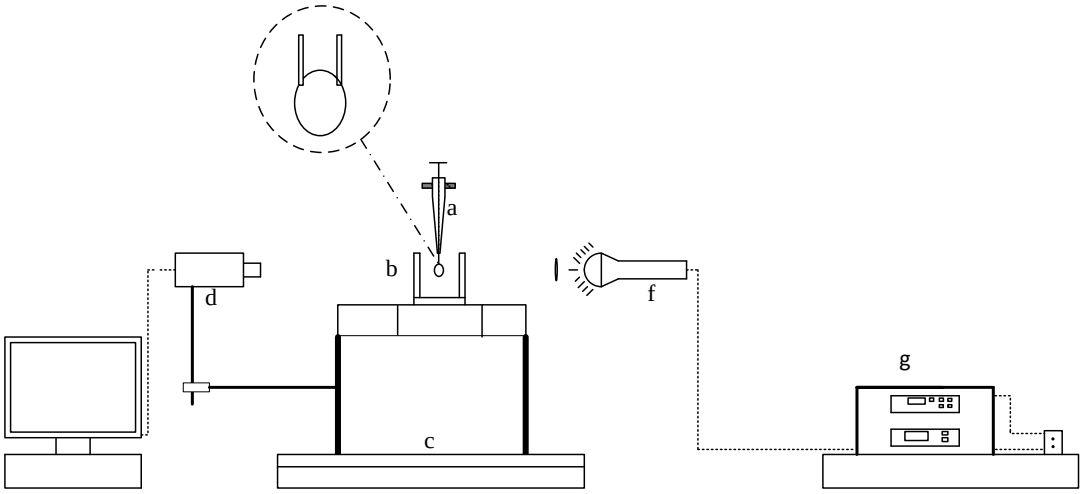

Figure 3-4: Pendant drop method setup: a. Syringe b. Cuvette c. Vibration proof table d. Camera e. Computer f. illumination system g. Electricity source

3.3.3 Solution Preparation and Surface Tension Measurement

The surfactants were weighed using a high precision balance. Stock solution was prepared using deionized water. For all experiments the stock solution is sonicated for half an hour to be certain that all surfactant fragments were dissolved. After which, all the surfactant concentrations were prepared from stock solution by dilution. To improve the accuracy, a smart needle was used to transfer stock dosage to dilution flasks. The solutions were under measurements directly after preparation. All experiments were run using an undisturbed surface area.

The dynamic interfacial tension measurements at the oil/water interface were conducted under conditions of room temperature and different molar ratios of surfactant using pendant drop. The syringe was loaded with surfactant solution and immersed in a cuvette of the alkane.

It is essential to prevent any potential evaporation of oil throughout the experimental time; we used a metal cap to secure the cuvette. The system was purged every time to avoid any air bubbles remaining in the tube at experiment time or during the change of surfactant concentrations. Syringe piston motion was extremely controlled to form a surfactant droplet with a diameter of 2mm of needle extremity.

Subsequently, the measurements were conducted at concentrations lower than critical micelles concentration (CMC). The equilibrium interfacial tension obtained as a function of interfacial tension regarding surfactants concentrations. In addition to that, sufficient adsorption time was allowed to verify equilibrium value. To avoid any contamination impacts on the interfacial tension measurements. All glassware and apparatus were well cleaned using Deconex 15E 6% by Volume.

3.4 Determination of interfacial tension at oil/water interface

The raw experimental results of dynamic and equilibrium interfacial tension were analysed sufficiently to be fitted by thermodynamic models later. To achieve that, the following programmes have been applied in sequence:

3.4.1 ImageJ Software

The movies that were captured for dynamic surface tension were converted to images using OGG software as depicted in figure (3-5a). ImageJ is defined as a processing programme that analyses the images by NIH image for Macintosh. The image undergoes to several processes after displaying such: editing, analysing, processing, saving and eventually printing in different bits (8,16,32). Furthermore ImageJ includes several formats: TIFF, GIF, JPEG, BMP, DICOM, FITS, in addition to raw [118].

In this study, TIFF format have been used together with 8 bits. It is essential to adjust drop image to ensure that the true-edge-on view is captured. A black colure offered by ImageJ as shown in Figure (3-5b) covers the whole image where the quality depends on enhancing the contrast. This procedure was repeated to include all targeted images which represent the dynamic curve stages. Then, the images were cropped at the appropriate scale to be compatible and to include all physical parameters (interfacial tension, area, curvature etc.).

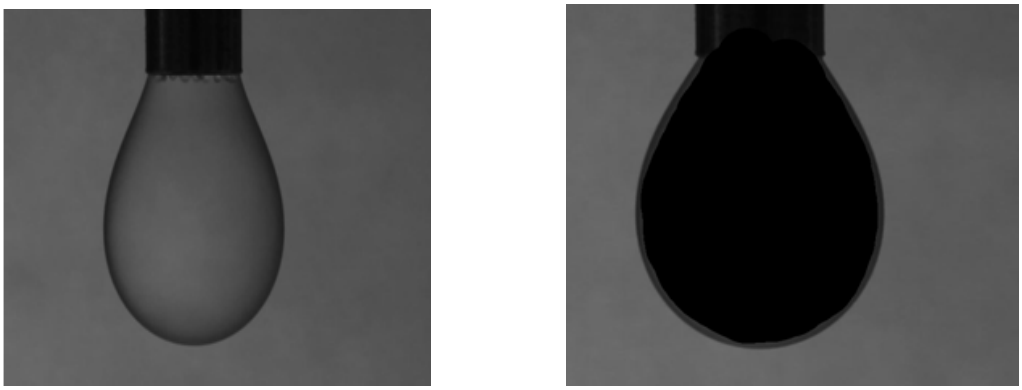

(a) (b)

Figure 3-5: Images of pendant drop; (a) raw image (b) image after processing by imageJ

3.4.2 Axisymmetric Drop Shape Analysis

Axisymmetric Drop Shape Analysis (ADSA) is a software developed to calculate the surface tension and contact angle of liquid / fluid interface regarding to the shape of axisymmetric menisci of pendant and sessile drops [119].

Two essential parameters are required for ADSA measurements, the outer diameter of needle and density difference between the fluids. Hence, the densities of both water and oil phases need to be measured beforehand by a density meter and computed into ADSA.

The scale factor of is calculated using following equation:

$$\text{Scal Factor cm/pix} = \frac{\text{Do}}{\sqrt{(Y2-Y1)^2+(X2-X1)}} \qquad (3\text{-}4)$$

Where D_0 is the external diameter of capillary nozzle in JSGC, and X, Y representing the two points in the nozzle edges.

Generally, ADSA was developed to implement all the characteristics related to pendant drop such as interfacial tension, volume, area and the radius of the cuvette at the apex. Figure 3-6 illustrate the steps of ADSA process.

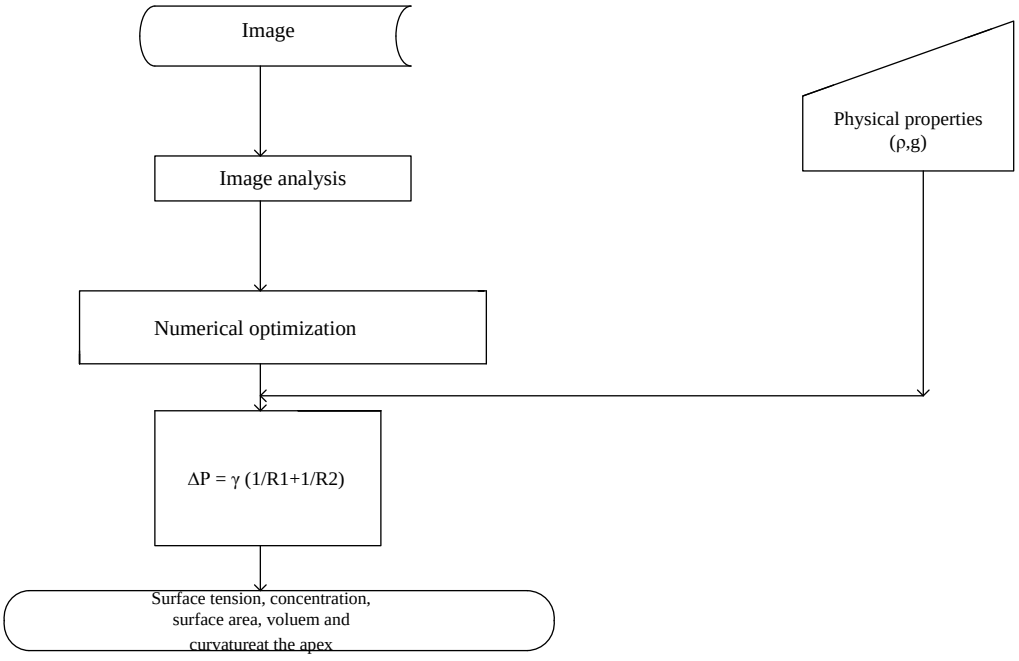

Figure 3-6: General procedure of Axisymmetric Drop Shape Analysis (ADSA)

To analyse the image of pendant drop, the image should be loaded into the software as shown in Figure (3-7). In this case, the analysis requires inputting parameters such as local gravity, a difference of densities between two applied phases, coordinates number of the image and scale factor. The principles of ADSA measurements depend on the shape of the drop.

Then, edge detection and smoothing is conducted where any remaining outliers are removed by applying second mentioned procedure as shown in Figure (3-8). The foundation of ADSA in measuring interfacial tension depends on a numerical procedure of fitting the experimental drop to the thermodynamic framework based on the Laplace equation. In fact, the accuracy of obtained interfacial tension returned to the consistency between the experimental and the theoretical curve.

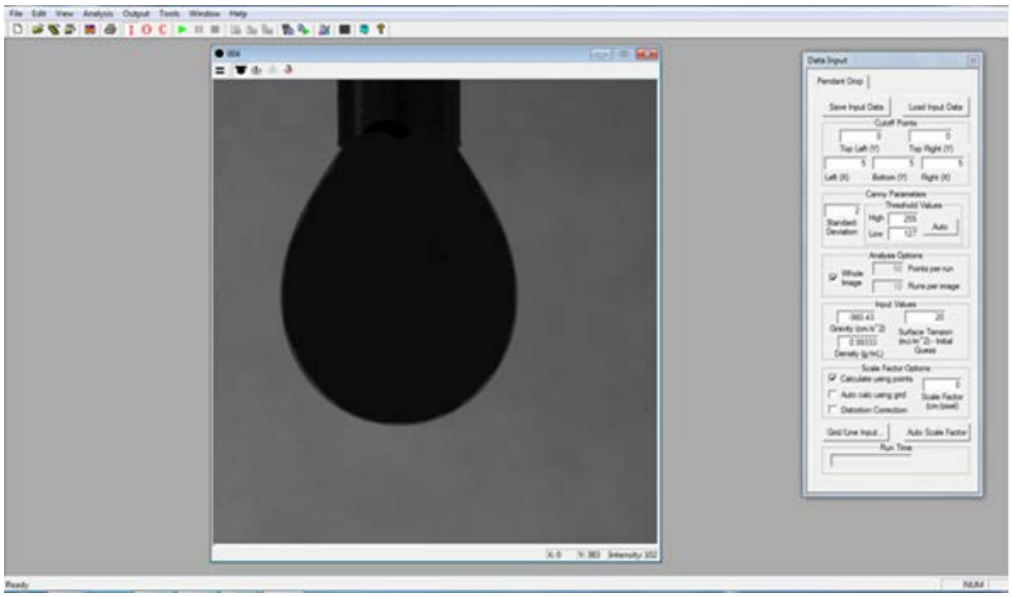

Figure 3-7: Image loaded to ADSA after processing by imageJ.

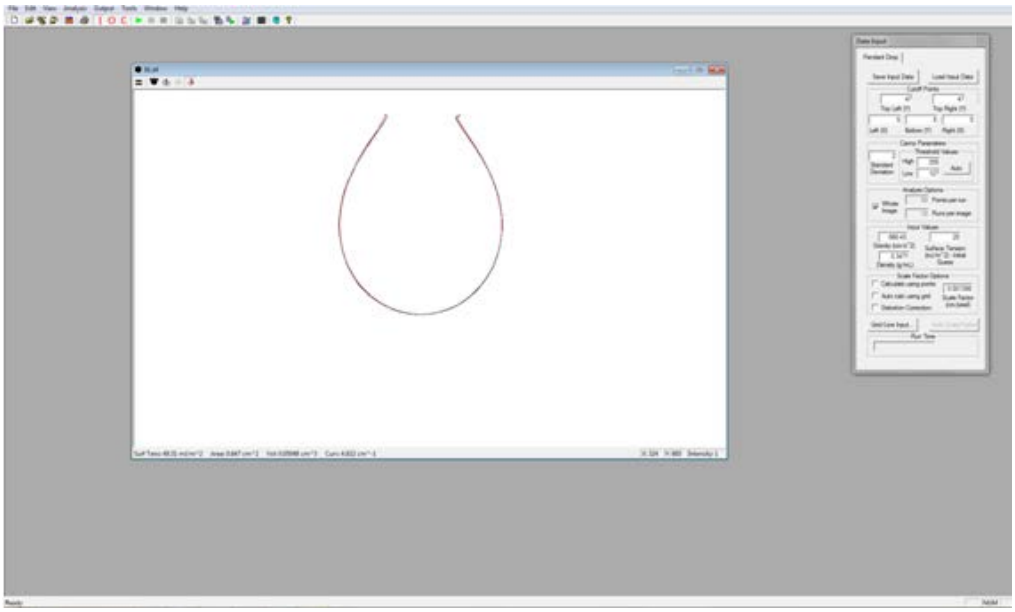

Figure 3-8: Consistency of theoretical and experimental curves at ADSA.

4 Dynamic adsorption of cetyl trimethyl ammonium bromide at alkane/water interface

4.1 Introduction

Experimental studies on oil/water interfaces have highlighted the distinguishing role of the oil molecules on the adsorption process. Experimental data with a variation in surfactant molecules or oil molecules have demonstrated the molecular origins of the interaction within the interface. For instance, results from a series of alkyle trimethyl ammonium bromide at hexane/water interface have demonstrated a competitive adsorption between short alkyl surfactants and hexane molecules [2].

Study of C_{10}TAB and C_{12}TAB with different alkanes (from octane totetradecane) also demonstrated the distinguishable impact of the oil molecules on interfacial adsorption [22]. Similarly, study on C_nTAB with hydrocarbons of same length indicated a strong dispersive force between surfactant and oil molecules [12]. Consequently, Fainerman et al. [23] proposed a new "binary" model, which included a new term accounting for the competitive adsorption between oil and surfactants molecules. The binary model has more fitting parameters than air/water interfacial model. However, the proposed model had the same quality of agreement with experimental data and thus cannot be justified from such data.

From reported values in the literature, there are variations in adsorption parameters for a common cationic surfactant, cetyl trimethyl ammonium bromide (CTAB) which attribute to limitations of applied theoretical framework. In spite of different parameters, all models provided a good fit to equilibrium data. A comparative study on different models have found that most models can fit the equilibrium data well [24] and good fitting cannot justify the underlying mechanism of the models.

In summary, the adsorption of CTAB has been studied in the literature by a number of researchers. While the experimental data were similar, the modelling results are different, depending on model assumptions. The non-unique values of the adsorption parameters render the procedure ineffective, especially for oil/surfactant interaction. The main deficit arose from the fact that the equilibrium data is too simple to distinguish the multiple effects on oil/water interfacial adsorption. The available

experimental data demonstrate a strong interaction between oil and surfactant at the oil/water interface. Yet, there is not effective method to quantify such effect. For this system, the current fitting procedure, which is solely based on the equilibrium data, is not sufficient to justify modelling assumptions.

Previously, our group has developed a new modelling approach to obtain the adsorption parameters from the dynamic, instead of equilibrium, surface tension [25]. By fitting simultaneously to two dynamic curves, i.e. dynamic surface tension at different concentrations, we were able to obtain unique modelling solution. The modelling framework is extended CTAB at oil water interfaces. In particularly, hexane and decane were used.

4.2 Experimental procedures

Several concentrations of cetyl trimethyl ammonium bromide have been prepared by deionized water. For completely dissolution of CTAB, the stock solution was continuously sonicated for more than 30 minutes. The other concentrations were prepared by dilution.

Before conducting the experiments with CTAB, every alkane was firstly tested by measuring surface tensions with pure water. The interfacial tension measurements start immediately after measuring surface tension of alkane and compare the results with literature. The volume needed to form the droplet for every concentration was exact measured before experiment starting.

The dynamic interfacial tension was conducted under sufficiently long time for every concentration. The experiment was achieved by emerging CTAB solution in a cuvette containing 30 ml of alkane. For every concentration, the syringe was well flushed by deionized water many times to avoid any remaining traces from previous concentration.

The camera is adjusted carefully by auto-focus on the droplet until image with clear edges has been obtained. It was critical to record the droplet under regular time without any disturbing. For this purpose, a stabilized table was used through all experiment time. It should be highlighted that unsuitable experimental conditions such disturbing formed droplet has negative influence on the measurements. This is

can be recognized on the curve of dynamic interfacial tension where affected area appears fluctuated before returns to stable mode.

The data has been analysis using following software's from image preparing until estimating final values of adsorption parameters: OGG Converter, ImageJ, ADSA, Excel and Excel solver. After the image is ready for analysis with ADSA, sequential images were used to get the value of dynamic interfacial tension.

All data is arranged in Excel sheet as following:

- Collecting row experimental data (frames, dynamic interfacial tension and time).
- The regression equation for every concentration was conducted (dynamic interfacial tension and $t^{0.5}$ to obtain γ_{eq}.
- Rosen approach has been used by applying Eq. (2-9)
- Applying Excel solver to do the fitting for experimental data of two concentrations simultaneously, and obtain adsorption parameters.

4.3 Results

4.3.1 Equilibrium interfacial tension

In this study, CTAB was used to measure the interfacial tension at different concentrations below critical micelles concentration (CMC). The measurements have been conducted on both hexane and decane/water interfaces. The experimental data was fitted using two different models: the conventional model and the new model.

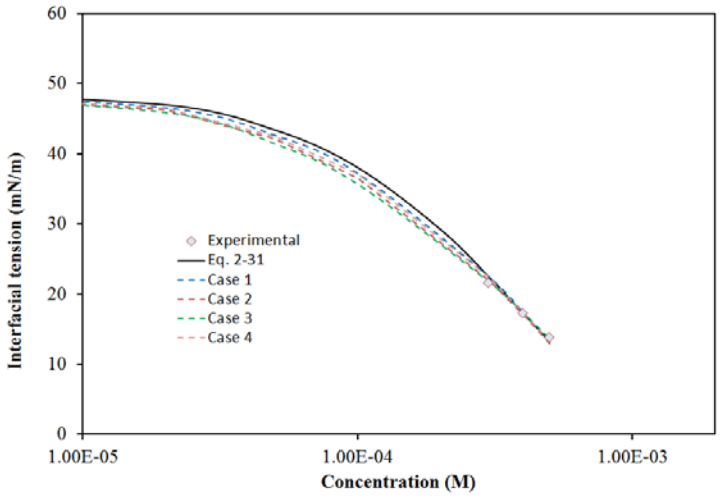

Figure 4-1: Equilibrium tension of CTAB at hexane/water interface

The first is conventional Szyszkowski, **Eq. (2-7)**, with different initial conditions, was applied to fit the data with K and Γ_m as adjustable parameters. The second is the new model, (**Eq. 2-31**).

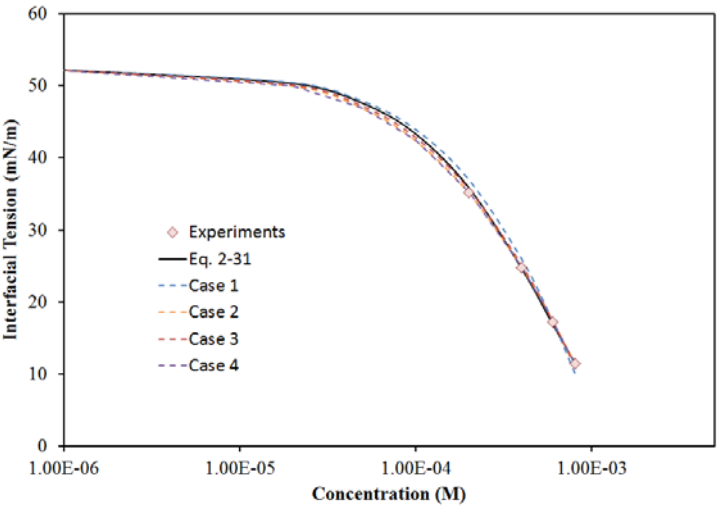

Figure 4-2: Equilibrium tension of CTAB at decane/water interface

The Excel solver was applying as shown in Figures 4-1 and 4-2, where small standard deviations were obtained for using Eq. (2-33) as listed in Tables 4-1 and 4-2 for the interfaces mentioned above. The best fitted parameters were determined by

minimizing sum of squares differences between experimental and modelling points. It can be seen that the two models can fit data very well.

However, Eq. (2-31) provided a unique solution. It can be observed that the value of new parameter χ varied widely between air/water and alkane/water interfaces as shown in Tables 4-1 and 4-2. This difference definitely is not related to the length of alkane chain as the value at hexane is higher than decane. The multiple best-fitting in Tables 4-1and 4-2 are expected given the variation in the literature. It should be noted all curves in Figure 4-1and 4-2 are indistinguishable even at the lower concentrations.

Table 4-1: Fitting parameters of CTAB at equilibrium of hexane/water interface.

Model	**Adjustable Variables**	**Best fitted Value**	δ_γ**(mN/m)**
New Model	χ (M-1) air/water [100]	747.06	**0.673**
	Hexane/water	2631.3	**0.503**
Szyszkowski Eq.			
Case 1	K (M^{-1})	7111	**0.453**
	Γ_m ($\times 10^6$ mol/m^2)	9.7	
Case 2	K (M^{-1})	8222	**0.269**
	Γ_m ($\times 10^6$ mol/m^2)	8.91	
Case 3	K (M^{-1})	5805	**0.579**
	Γ_m ($\times 10^6$ mol/m^2)	0.108	
Case 4	K (M^{-1})	9909	**0.128**
	Γ_m ($\times 10^6$ mol/m^2)	8.1	

Table 4-2: Equilibrium fitting parameters of CTAB at decane/water interface.

Model	Adjustable Variables	Best fitted Value	δ_γ(mN/m)
New Model	χ (M^{-1}) air/water [100]	747.06	0.673
	χ (M^{-1}) Decane/water	1883	0.465
Szyszkowski Eq.			
Case 1	k(M^{-1})	2300	1.07
	Γ_m($\times 10^5$ (mol/m^2)	1.63	
Case 2	k(M^{-1})	4500	0.53
	Γ_m($\times 10^5$ (mol/m^2)	1.08	
Case 3	k(M^{-1})	3770	0.27
	Γ_m($\times 10^5$ (mol/m^2)	1.19	
Case 4	k(M^{-1})	4354	0.023
	Γ_m($\times 10^5$ (mol/m^2)	1.10	

Using the conventional model would provide multiple combinations of K and Γ_m. Details of the fitting can be found in **Appendix 1**. Such non-unique results would make the impossible to get the appropriate values for dynamic modelling. The new equation, on contrast, had a single fitting parameter and produced a unique fitting. The results from the new model will be used for dynamic modelling. In the other words, the equilibrium data is insufficient to verify the adsorption constants.

4.3.2 Dynamic interfacial tension

The adsorption kinetic at oil/water interface followed a slow process with gradual reduction. Due to the experimental procedure, no effective data was obtained before 1 s. Nevertheless, the data is sufficient for dynamic modelling (Fig. 4-3 and 4-4). For hexane Two concentrations, 0.3and 0.5 mM, were fitted simultaneously (solid lines) and gave good fitting for the dynamic model. In addition, 0.2 and 0.6 mM were selected for fitting at decane/water interface. The coding for numerical model can be found in **Appendix 3.**

The dynamic modelling resulted in adsorption were maximum surface excess Γ_m and affinity constant *K*. The standard deviation of both interfaces was less than1 mN/m with 0.371 and 0.313 for 0.3 and 0.5 mM at hexane. Whereas at decane read 0.572 and 0.340 mN/m for 0.2 and 0.6 mM respectively. These fitting deviations agreed with standard errors in literature, and can be classified as excellent fitting [6].

Furthermore, the model was used to predict the data at 0.4 mM (hexane) and at 0.4 0.8 mM at decane interfaces. The standard deviations of the prediction were also smaller than1 mM/m and indicated excellent predictability.

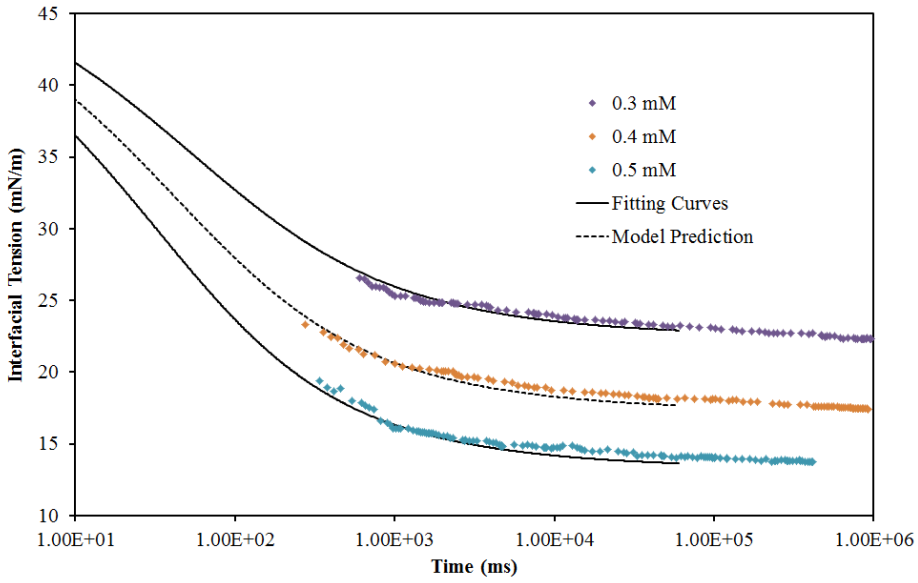

Figure 4-3: Dynamic interfacial tension of CTAB at hexane/water interface.

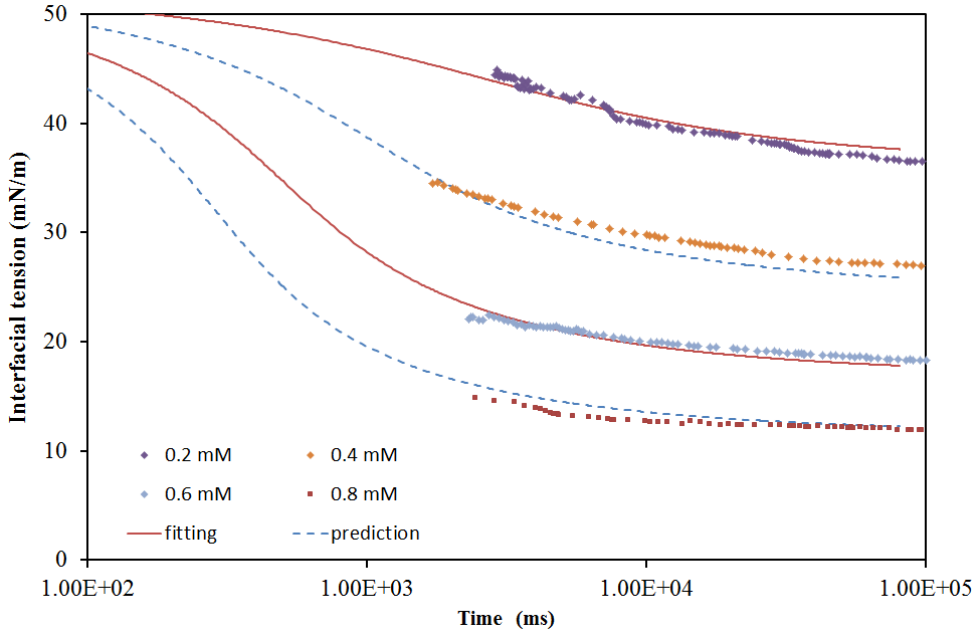

Figure 4-4: Dynamic interfacial tension of CTAB at decane/water interface.

As mentioned the new model was applied on two concentrations where the standard deviation for all dynamic curves were consist with theoretical standards.

4.4 Discussion

4.4.1 Comparison with literature values

As mentioned earlier, CTAB adsorption has been reported many times in the literature. For instance, the variations in adsorption parameters for adsorption at water/hexane interface are presented in Table 4-4. In spite of different parameters, all models provided a good fit to equilibrium data. The reported values varied widely from 2.38 to 3.13 × 10^{-6} mol/m^2.

Table 4-3: Adsorption parameters of CTAB at hexane/water interface.

Γ_m (mol/m^2)	K (M^{-1})	Model	Reference
2.38×10^{-6}	1.5×10^{7}	FC	[2]
2.63×10^{-6}	2.2×10^{7}	FIC	[2]
3.13×10^{-6}	120×10^{5}	Binary model	[23]
2.38×10^{-6}	1.6×10^{7}	LC	[20]
2.61×10^{-6}	2.2×10^{4}	FIC	[20]

On contrast, the data from dynamic modelling is fundamentally different. The physical quantities which were determined from the new dynamic model are presented in Table 4-5 in comparison with those at air/water [85].

Table 4-4: Adsorption parameters of CTAB at different interfaces.

Interface	**Γ_m (mol/m^2)**	**K (M^{-1})**
Air/water	6.32×10^{-6}	2017
Hexane/water	7.15×10^{-6}	1237
Decane/water	10.22×10^{-6}	9600

The experimental data was well described by the new model, for both fitting and predicting curves. This experimental data was similar to previous data in literature [7]. However, the modelling results are fundamentally different, especially in terms of Γ_m which is directly linked to the structure of interface zone.

It is important to note that by applying to two concentrations simultaneously, the dynamic modelling gives unique values of *K* and Γ_m. The obtained Γ_m is high for hexane and decane/water interfaces (Table 4-5). However, this is not outside the typical range for surfactants, which were obtained from the equilibrium fitting [6]. In summary, the data from this study is unique for equilibrium tension and more consistent for dynamic tension.

4.4.2 Influence of oil molecules

At hexane interface, the value of Γ_m is a bit higher than air/water interface and provides implicit subscription of oil molecules in the interaction at adsorption layer. As the alkane chain length increased (decane) the interactions also increased, and as result the value of Γ_m has almost doubled from the air/water interface.

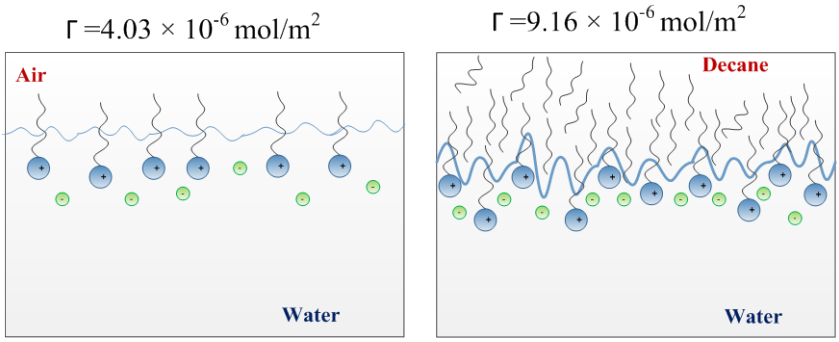

Figure 4-5: The arrangement of CTAB molecules at: air/water and decane/water

To interpret that the predicted Γ at the CMC were obtained at decane/water interface and compared to air/water interface: Γ_{CMC} was 4.03 and 9.16×10^{-6} mol/m^2 at air and decane/water interfaces, respectively. The increment is consistent with the proposed increment of surfactant at the oil/water interface. For instance, it has been found that SDS adsorption can increase as much as 13 times from air/water to alkane/water interface [41]. The result indicates a structural variation within the adsorption zone. For air/water interface, the CTAB packing is limited by electrostatic repulsion between the heads (Fig. 4-5a).

Structure layer of aqueous solution at air/water interface forms monolayer at limitation of 8×10^{-6} mol/m^2 [6]. The saturated monolayer packing, assuming that the trimetyl ammonium heads are in the same horizontal plane, was 6.2×10^{-6} mol/m^2 [120]. In the other words, the obtained Γ_{CMC} in this study is greater than the limitation of mono-layer proposed in literature.

The results at decane/water interface demonstrated that CTA^+ heads are not in same plane (Fig. 4-5b). The bromide Br^- ions with high diffusion coefficient play a significant role in interfacial area and built layers around head group. This sort of arrangements assist to make CTA^+ molecules pack closer more than air/water and of

course leads to high Γ_m. Furthermore, the arrangement of Br^- ions consider hypothesis and as result repulse with water molecules because they are not dissolve in water system. It is interesting to refer that the high density of CTA^+ tail, breach mentioned system and provide a path for Br^- ions to close the surface [100]. At oil/water interface the thickness of surfactants layer probably return to interface fluctuations. Depending on this figure, the roughness of surface is also expected where the oil layer has thickness [104]. The proposed mechanism is consistent with the increased thickness of the decane/water interface, as showed by X-ray study [105]. Neutron reflectometry also demonstrated that the oil/water inter-facial thickness is 3 times thicker than air/water interface [104]. Due the presence of oil molecules of hexane and decane, the oil/water interface produces additional volume that is available for CTA^+ molecules. Furthermore, the repulsive force, between dodecyl tail of CTA^+ and decane molecules, can balance the electrostatic force and disrupt the monolayer arrangement. This arrangement is similar to Ivanov's proposed arrangement [67].

In summary, the obtained data demonstrated the significant role of oil molecules on the adsorption layer of CTAB. It can be deduced that CTA^+ molecules are not at same level due to the roughness of layer adsorption, which means the surfactant followed a multi-layers arrangement.

4.5 Summary

In this study the behaviour of CTAB solutions at the hexane and decane/water interfaces were investigated using pendant drop method. The experimental data was effectively modelled at equilibrium by a simple model with one parameter which offers one solution.

The results demonstrated the success of new model in describing data. In addition, experimental results at equilibrium were also modelled using the Syszkowski equation where multiple solutions have been obtained. Consequently, the new model was also applied at dynamic conditions to fit two concentrations simultaneously.

The results exhibited consistency between modelled and experimental data. The obtained parameters indicated a fundamental difference between air/water and

oil/water interfaces: the adsorbed quantity increased significantly. In case of decane, the adsorption concentration was double. The difference reflects the critical impact of hydrophobicity of hexane and decane molecules on the adsorption layer.

The study verified to the participation of hexane and decane in the adsorption process. Hence, the surfactant inter-action is no longer dictated by electrostatic force between surfactant heads and counter-ions. The repulsion between oil and surfactant tails also plays a critical role.

5 Adsorption dynamics of Gemini surfactant at decane/water interface

5.1 Introduction

Gemini surfactants are well known by their special structure that consists of two hydrophilic head and two hydrophobic chains with a spacer in between [47-49]. Most of Gemini surfactants possess symmetrical structures and refer as m-s-m where m is the carbon atoms number in the two tails and s is the number of carbon atoms in the spacer. Furthermore, some Gemini surfactant s have more than two heads and tails and sometimes different tail length and known as unsymmetrical Geminis [51-55].

In comparison to their conventional surfactants, Gemini surfactants have superior properties which influenced by length of spacer group, hydrophobic chain length and dissymmetry. Their unique surface active characteristics have attracted considerable interest. One of these features is the observed low critical micelles concentration [30]. Furthermore, the viscosity of aqueous Gemini surfactants with short spacer is much higher to monomeric analogue surfactants at low concentrations and excellent efficiency in reducing the interfacial tension [30, 56-62].

Despite of important applications of different industrial and scientific fields, there is lack and shortage knowledge in investigating the dynamics and kinetic characteristics of Gemini surfactants. One of the main controversial issues regarding Gemini surfactant is the value of ionic constant in Gibb equation, Eq. 2-3. The conflicting reports have been critically reviewed by Zana [30]. At this stage, there is no consensus regarding the value of *n*: some researchers select *2*, while other selected *3*. More extraordinarily, neutron reflectometry indicated that *n* varies with concentrations [121]. By modelling from dynamic tension, the fitting can circumvent the Gibbs equation and controversies regarding *n*. Such advantage has been demonstrated in a recent study with a Gemini surfactant at air/water interface [101].

In this study, the dynamic and equilibrium interfacial tension of Gemini cationic surfactant α,ω-bis (N-alkyl dimethylammonium) were investigated using pendant drop method.

5.2 New theoretical framework

In this study, a new modelling approach was developed to fit the experimental data of Gemini surfactants at oil/water interface. It is well known that Gibbs adsorption equation is essential approach and pivotal to predict the adsorption of surfactants at several different interfaces addition to many applications in technical and industrial fields. In this study, these thermodynamic frameworks were characterized without Gibbs equation. These new models showed sufficient powerful capability on describing different data of dynamic and equilibrium tensions.

Many attempts have been done to fit the full experimental data of Gemini surfactant using mentioned model of Eqs. (2-31) and (2-32), addition to the extended model that was used to improve the fitting data of Gemini surfactant (C_{12}-C_3-C_{12}) at air water interface [101]. However, applying these models deficit to provide sufficient fitting and exhibit a real gab between experimental results and theoretical models [55]. The new equation for CTAB, that is Eq. 2-31, was also applied without success.

Accordingly, a new mathematical approach was exclusively developed for Gemini surfactant to replace the Eq. (2-31). The equation for Gemini surfactant is given as following:

$$\gamma_{eq} = \gamma_0 - (\gamma_0 - \gamma_{min}) \frac{Q_{eq} c_b}{1 + Q_{eq} c_b} \qquad (5\text{-}1)$$

Where, γ_{min} is the minimum interfacial tension (mN/m) and Q_{eq} is new equilibrium constant (M^{-1}). These parameters are adjustable parameters and can be used to predict the dynamic adsorption. Hence equation (5-1) is extended to the dynamic relationship:

$$\gamma(t) = \gamma_0 - (\gamma_0 - \gamma_{min}) \frac{Q_{eq} c(t)}{1 + Q_{eq} c(t)} \qquad (5\text{-}2)$$

This model provides a well description for the experimental results as can be explained later. It is worth to mention that, Eq. (5-1) has the same characterization of Eq. (2-31) where one can see that the adsorption density is not included in the equation and there is direct relationship between interfacial tension and bulk concentration. Consequently, Eq. (5-2) was replaced by Eq. (2-32) and success to calculate the dynamic interfacial tension for all Gemini concentrations. In addition, the new model approach does not require Gibbs adsorption isotherm and does not affect with any variance that may occurs in the thickness of sub-surface concentration. It should be noted that Equation (5-1) was inspired by the Rosen's approach, i.e. equation (2-9).

5.3 Experimental procedure

The dynamic and equilibrium interfacial tension of Gemini surfactant have been conducted by applying the same procedure of conventional surfactants at chapter 4. It should be mentioned here that the concentrations of Gemini surfactant were prepared at concentrations lower than those conducted at conventional surfactants.

5.3.1 Gemini surfactant synthesis

The Gemini surfactant of type m-s-m was eventually formed as depicted in **Figure 5-1.** The synthesis reaction was verified as illustrated briefly in the following procedure: all synthesis reactions were conducted under a positive pressure of dry nitrogen in oven-dried glassware. Commercially available solvents and reagents were used as purchased from Sigma-Aldrich. All NMR experiments were performed on a Bruker AVANCE III 400 MHz spectrometer at 298K.

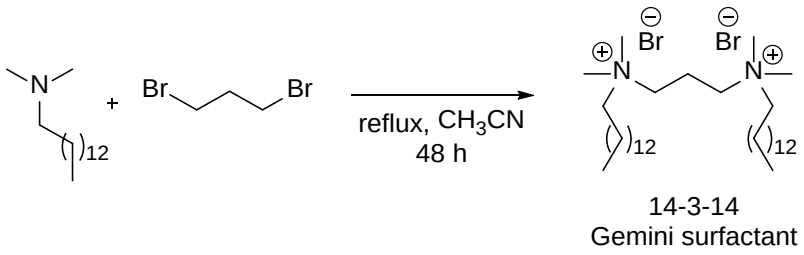

Figure 5-1: Reaction synthesis of Gemini surfactant (C_{14}-C_3-C_{14}).

To achieve the synthesis reaction we used a 250 mL round-bottom flask fitted with a reflux condenser and a magnetic bar was added N,N-dimethyltetradecylamine (24.15 g, 0.1 mol), 1,3-dibromopropane (10.09 g. 0.05 mol) and acetonitrile (80 mL). The reaction mixture was heated to reflux with vigorous stirring for 48 h. Then the mixture was subsequently cooled down slowly to 0 °C, upon that a white precipitate formed. The white solid was filtered and wash with acetonitrile (3 x 30 mL). Recrystallization of the solid product from boiling acetonitrile resulted in the C_{14}-C_3-C_{14}. Gemini surfactant was obtained as a white solid. The product was analytically pure as confirmed by ^{1}H-NMR spectroscopy.

It should be noted that this Gemini surfactant was selected after some initial testing. The dynamic surface tensions were obtained in the reasonable range, from 10 s to minutes, for the effective dynamic modelling. On contrast, the dynamic adsorption of C_{12}-C_3-C_{12} was too fast and thus was not used in this study.

5.3.2 Estimation of CMC

The CMC of C_{14}-C_3-C_{14} was determined in this study by measuring the interfacial tension at varied concentrations. Therefore, the titration of dynamic interfacial tension has been applied to measure CMC of C_{14}-C_3-C_{14} and found to be 0.13 mM which is consider in consistency with literature value of 0.15 mM [65]. This low of CMC value regarding to conventional surfactants can return to the time that two alkyl chains of C_{14}-C_3-C_{14} take to move from water to micelles pseudo phase [122].

5.3.3 DOSY-NMR experiment to determine the diffusion coefficient

In general, useful information about surfactants geometric characteristics in solutions can be obtained by self-diffusion measurements using nuclear magnetic resonance (NMR). These measurements have a wide range of applications such, DNA, protein properties, and self-diffusion coefficients. There are several experimental procedures that widely used to determine the diffusion coefficient of bulk solution such as NMR spectroscopy [123], longitudinal encode-decode LED [124] and BPP-SED [125].

As can be seen in Figure 3-7 the ^{1}H NMR spectrum of (C_{14}-C_3-C_{14}) has been performed in D_2O where the single was suppressing by WATERGATE pulse

sequence. Proton NMR self-diffusion experiments were carried out using a Bruker AVANCE III NMR spectrometer at 400.13 MHz. The surfactant sample of 1mM was prepared by D_2O and placed in 5mm NMR test tube therewith put in the apparatus for measurement. All measurements were carried out in controlled temperature (25 °C) and in consideration to weaken single of water we sued D2O instead of water. The 2D DOSY experiments were performed using standard Bruker pulse sequences (*ledbpgp2s*) which employs longitudinal eddy current delay (LED) with bipolar gradient pulse pair and 2 spoil gradients. The bands of resonance were seen at 0.835, 1.258 and 3.187 ppm which based on methylene protons. The single peak of resonance at 3.187 ppm is related to methyl protons escorted by hydrogen molecules.

The δ (the gradient duration) and Δ the diffusion coefficient (the time intervals between pulse onset) values were optimizes for every concentration (using the 1D pulse sequence *ledbpgp2s1d*, δ (2×P30) and Δ (d20), Bruker's TopSpin). The diffusion experiments were recorded with δ = 2000–3000 μs, Δ = 100 ms, eddy current delay (D21) = 5 ms, and 16 scans per spectrum. The data were processed by Bruker's TopSpin which immediately shows the diffusion coefficient *D*.

Herein the echo multiple was applied due to the diffusion time to quantify the relationship between gradient pulses and accordingly the gradient strength. In their pioneer work, Stejskal- Tanner [126] proposed pulsed gradients to the spin of echo sequence, and that is provide better results in comparison to previous study. They provide a solution of partial differential equation of Bloch-Torry and introduce the following formula:

$$\ln\left(\frac{I}{I_0}\right) = -\zeta^2 g^2 D \delta^2 \left(\Delta - \frac{1}{3}\delta\right) \qquad (5\text{-}3)$$

Where ζ is the gyromagnetic ratio of the proton, I is the amplitude of echo signal I_0 is the amplitude when g=0, g is the strength of gradient pulse. Therefore, to determine

the diffusion coefficient *D* the data was fitted by applying mentioned equation and fitted function curve that calculated by ^{1}HDOSY is illustrated in Figure 5-2.

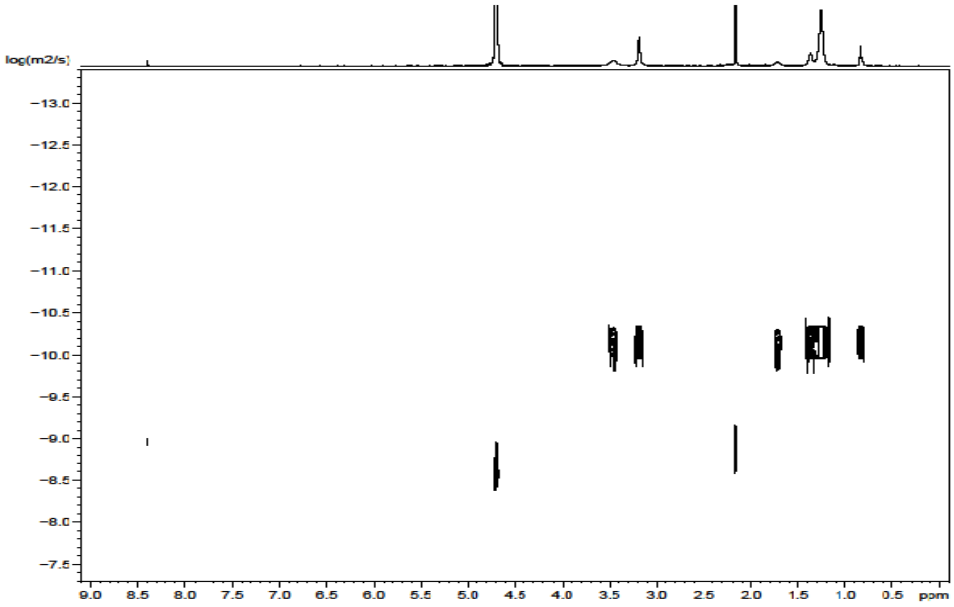

Figure 5-2: H NMR experiment to measure diffusion coefficient (spectrum with D_2O suppressing in C_{14}-C_3-C_{14})

Depending on the calculations of function fitting curve (Fig. 5-3), it has been detected that the diffusion coefficient value was 6.0×10^{-11} m^2/s. This value will be used later in the dynamic modelling.

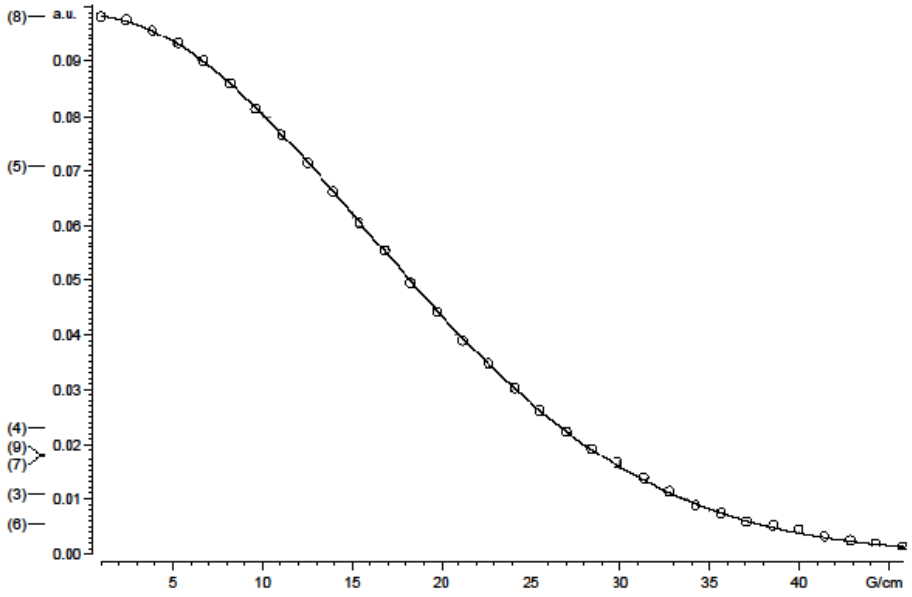

Figure 5-3: H NMR measurement (fitted function curve)

5.4 Modelling results

5.4.1 Equilibrium interfacial tension

The equilibrium interfacial tension was measured for a series of aqueous solution of surfactant at concentrations less than CMC as shown in Fig. 5-1. Consequently, Eq. (5-1) has been applied to fit experimental results where the model success to provide good fitting as shown in Fig (5-4).

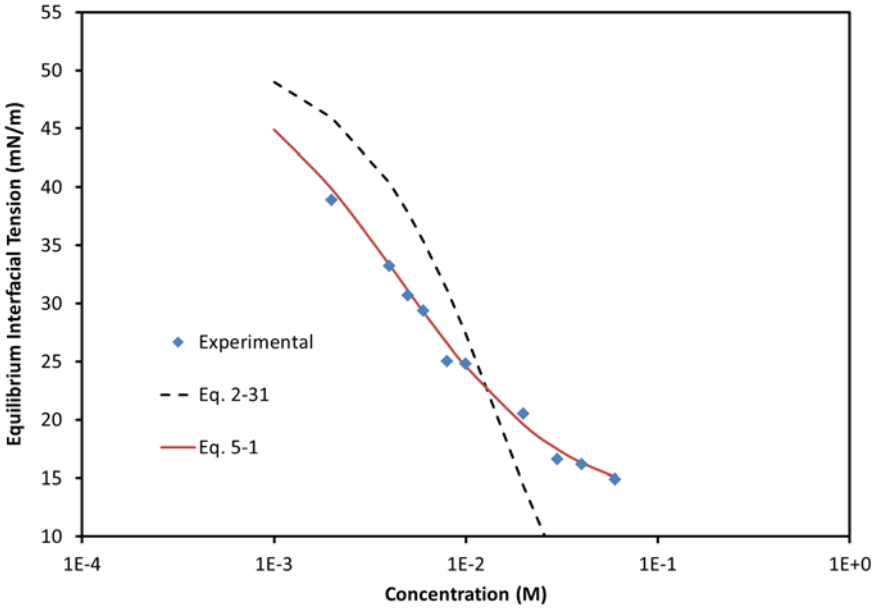

Figure 5-4: Modelling equilibrium interfacial tension

The adsorption parameters of new equilibrium model were changed several times to verify the best equilibrium fitting and used as initial values to promote dynamic fittings. The deviation between experimental data and modelling results are less than 1 as shown in Table 5-1, and considered as acceptable deviation [127].

The best-fitting values from the new thermodynamic model (**Eq. 5-1**) are obtained as following:

$\underline{Q_{eq}}$= 226710 M^{-1} and γ_{min} = 12.34 mN/m

The behaviour of equilibrium adsorption of C_{14}-C_3-C_{14} is similar to other results [74]. The surface tension of Gemini surfactant follows the concave and convex region. Hence, two-parameters fitting were needed.

Table 5-1: Experimental and modelling results of equilibrium adsorption (γ_0=52.3 mN/m)

No	Concentration (mM)	Experimental IFT (mN/m)	Fitted value (mN/m)	Deviation (mN/m)
1	0.000	52.30	52.30	0.000
2	0.004	33.20	33.29	0.0086
3	0.005	30.68	31.07	0.1490
4	0.006	29.37	29.27	0.0111
5	0.01	24.80	24.57	0.0543
6	0.02	19.62	19.56	0.0044
7	0.03	17.64	17.46	0.0335
8	0.04	16.15	16.30	0.0218
9	0.06	14.86	15.07	0.0418
				0.3246

5.4.2 Dynamic interfacial tension

The fitting of experimental data of C_{14}-C_3-C_{14} at decane/water interface exhibits unusual behaviour, with complicated dependence on the concentrations. It should be noted that the dynamic adsorption of C_{14}-C_3-C_{14} is much longer than that of CTAB, which was caused be low diffusion coefficients and complicated adsorption kinetics. Thus the molecular interactions at interface adsorption layer became more dominant.

In the literature, there are several observations on experimental results of Gemini that require different thermodynamic framework [30]. In this study, two thermodynamic models have been used to describe the adsorption at different concentrations. The dynamic fitting procedure has conducted by applying two concentrations simultaneously. The *s*- shape of dynamic adsorption of C_{14}-C_3-C_{14} has complete elements that have been mentioned by Rosen's qualitative description (Chapter 2). For this surfactant, the two modellings are based on: (i) Langmuir adsorption

isotherm with two fitting parameters (k_L, Γ_m) and (ii) Frumkin adsorption isotherm with three parameters (k_F, Γ_m, A).

A. Langmuir adsorption isotherm

The same numerical solution has been applied to solve Eqs. (2-5) and (2-19) where the value of sub-surface concentration $c_s(t)$ is used to calculate interfacial tension at Eq. (5-2). Langmuir model failed to describe the adsorption behaviour at very low concentrations [128, 129]. This model is most frequently used isotherm due to its simplicity, and provides some of key physics at adsorption layer. The model ignores inter-molecular interaction between adsorbed molecules, such as electrostatic interactions or intra-monolayer interactions. In other words, the reduction in the curve is only governed by the lateral attractions. In this regard this model has been used to model the experimental data of higher concentrations (0.02, 0.03 and 0.06 mM). The adsorption parameters of adsorption fitting are listed in Table 5-2, and the best fitting was basically obtained by determining the less standard deviation for applied concentrations.

Table 5-2: Adsorption parameters obtained by the best fit of Langmuir model.

c_b (mM)	K_L (M^{-1})	Γ_m (mol/m^2)	A	δ_γ
0.02 - 0.03	603676	2.12×10^{-6}	0	(0.93 & 0.52)
0.02 - 0.06	603676	2.20×10^{-6}	0	(0.88 & 0.42)

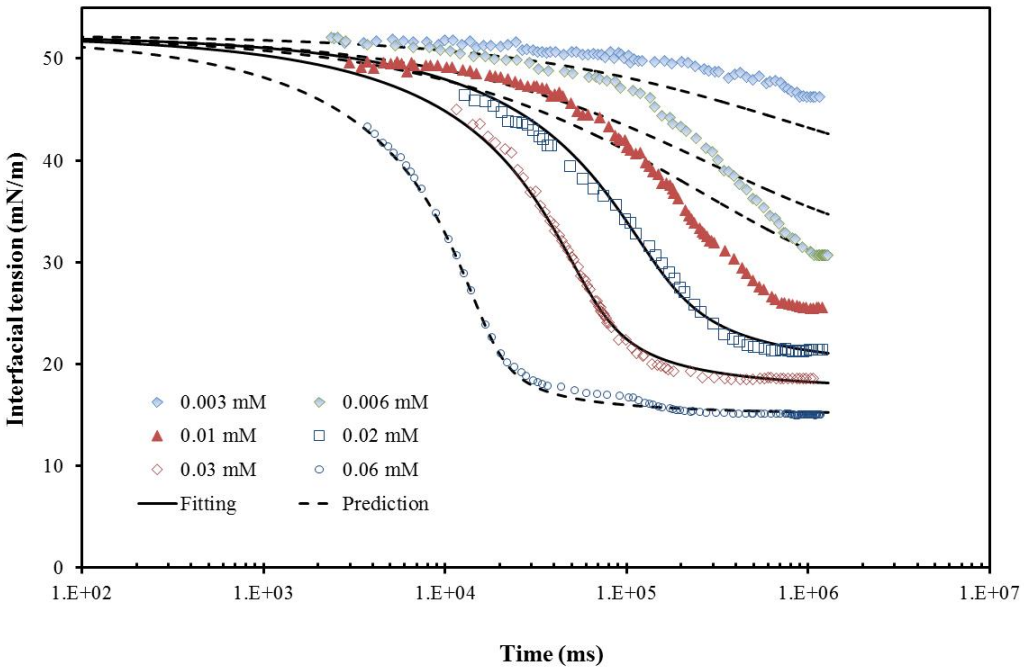

Figure 5-5: Dynamic interfacial tension, fitting at 0.02 and 0.03 mM.

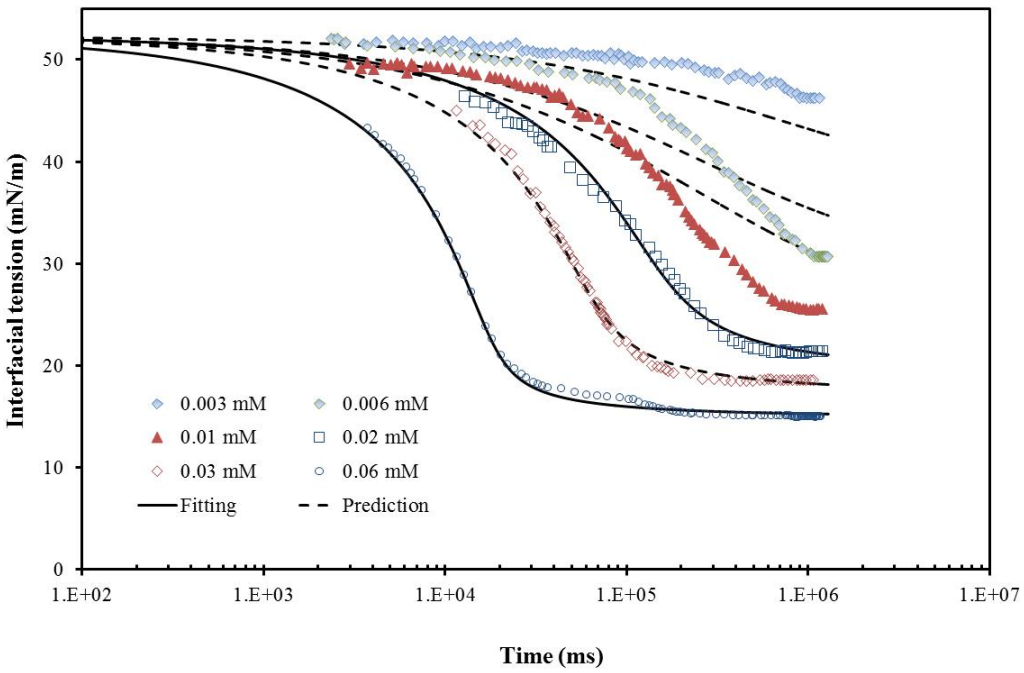

Figure 5-6: Dynamic interfacial tension, fitting at 0.02 and 0.06 mM.

The fitting results can be seen in Figures 5-5 and 5-6. At higher concentrations, the model exhibits capability to fit the results. The results come with good standard deviation in spite of few deviation points (as shown in at the beginning of curve 0.03 mM of Fig 5-3). These deviations may attribute to potential errors that may occur through the measurements. It should be mentioned that the best results for Langmuir model is at (0.02-0.06 mM) regarding to smallest deviations (Table 5-3).

Consequently, it is clear from the results that the condition is diffusion–controlled and the kinetic step is not needed. However, the model could not fit the low concentrations (<0.01 mM). At the low concentrations, the modelled predictions are slower than experimental values. Hence, the Frumkin isotherm was employed to deduce surfactant behaviour at low concentrations. In this instance, the model have an additional parameters, *A*, and thus became more flexible.

B. Frumkin adsorption isotherm

The dynamic model, with numerical solution to solve Eqs. (2-8) and (2-19), was applied to obtain $c_s(t)$. Consequently, $c_s(t)$ was used to obtain dynamic interfacial tension and fitted against the experimental results at low concentrations.

In the literature, Frumkin isotherm is typically used to include interaction between surfactant molecules. In addition, it was found these interactions take long time before equilibrium adsorption can be established [77]. The fitting results of dynamic interfacial tension by applying Frumkin model are depicted as full plotted curves in (Fig. 5-2). Two concentrations 0.001 and 0.01 mM simultaneously (solid lines) and provide good fitting for dynamic adsorption. The adsorption parameters are listed in Table 5-3, (including Γ_m, k, A, δ_γ and concentrations).

Table 5-3: Adsorption parameters obtained by the best fit of Frumkin model.

c_b (mM)	K_F (l/mol)	Γ_m (mol/m^2)	A	δ_γ	Quality of fit
0.003-0.01	120901	7.954×10^{-6}	-6.28	(0.304&0.600)	Good

It can be seen that the Frumkin model described appropriately the experimental data and provides better fitting for 0.01 and 0.001 mM curves, due to additional parameter *A*. Negative value of *A* refers to the spontaneity of adsorption process.

This can be explained in terms of shortage of polar groups on hydrophobic alkyl chain of surfactants which results in more impacted contact between surfactant molecules. The resulted curves seem to be steeper than Langmuir isotherm for positive *A* (attraction between molecules). Also, the curves are steep (low concentration) and inclined to be straight at 0.001 mM. Nevertheless, the curves fail to predict at other concentrations.

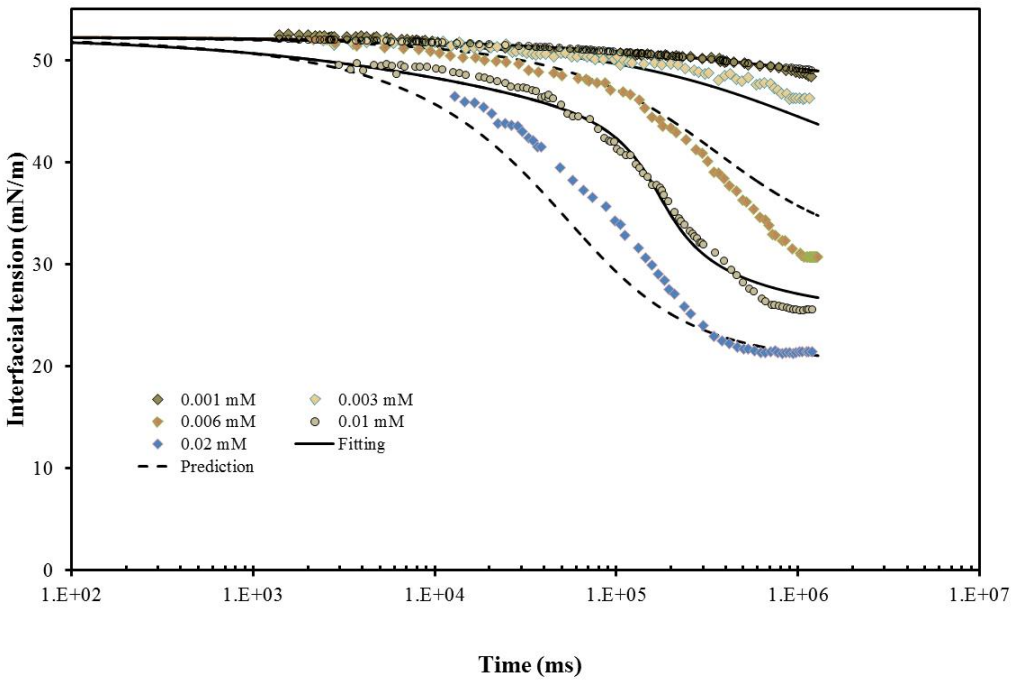

Figure 5-7: Dynamic interfacial tension (0.003 & 0.01 mM)

5.5 Discussion

5.5.1 Equilibrium tension

In this regard, the researches on dynamic modelling of Gemini surfactants are scarce, in comparison with conventional surfactants. Finding an appropriate theoretical model, that can describe adsorption dynamically, remains difficult. Instead, many

researches have proposed the conflicting hypotheses about the interfacial structure and ionic bounding of Gemini surfactants.

This study modelled the dynamic and static adsorption of experimental data of Gemini surfactants with a new theory. The theory is more reliable than conventional methods in obtaining adsorption constants. The equilibrium experimental data of C_{14}-C_3-C_{14} was modelled by applying new model Eq. (5-1). As illustrated in Figure (5-4), it is clear that this model provided very good fitting to experimental results. It should be highlighted that there are two parameters involved in this model instead of one as mentioned in Eq. (2-31) (Chapter 4).

The first adjustable parameter is minimum interfacial tension γ_{min} between oils and surfactant solutions. This term has been mentioned in literature[130], in similar situation between salts concentrations and different oils. In fact, there is similarity between minimum interfacial tension γ_{min} and the interfacial tension at CMC (γ_{CMC}) and critical aggregate concentration (γ_{CAC}). In this regard, γ_{CMC} becomes γ_{min} and the slope gradually turns to zero, instead of a sudden change as with conventional surfactants [131]. The second parameter is the new Gemini adsorption constant Q_{eq} which has the same origin as χ in Eq. (2-31). These parameters have been used to obtain better equilibrium fittings and in turn were applied for dynamic modelling. Accordingly, Eq. (5-1) provides an appropriate and implicit prediction for equilibrium curve. The implicit nature of the equation is the key for dynamic modelling.

5.5.2 Dynamic tension

In literature, the majority of modelling results that concern about determining of adsorption constants of surfactants were based on equilibrium data with uncertainties. In this study, our new mathematic model (Eq. 5-2) was used to model experimental data at different concentrations. The new theoretical model interpreted the dynamic adsorption is dominated by diffusion and therefore the kinetic step is not required.

Generally, the adsorption of C_{14}-C_3-C_{14} is to be more effective at oil interface [75]. Physically, equilibrium adsorption of C_{14}-C_3-C_{14} (Fig. 5-1) is very slow comparing

to our results on conventional surfactants at Chapter 4 and consider similar to equilibrium adsorption of Gemini surfactants at oils interfaces as reported in literature [74].

Interestingly, the dynamic adsorption of C_{14}-C_3-C_{14} exhibits unusual response for the theoretical fittings, depending on the concentrations. Langmuir isotherm was only successful to predict the dynamic adsorption at the higher concentrations. The failure of the Langmuir isotherm at lower concentrations is apparently originated from molecular structure of the Gemini surfactant.

Consequently, to improve the fittings, Frumkin isotherm model has been proposed. The new fitting becomes more flexible with 3 parameters (Γ_m, k, and A). The model can improve the fitting but not overall predictions (i.e. at all concentrations). The non-ideality parameter A was suggested by Frumkin to calculate the interactions between surfactants molecules. From the value of A, the interaction between molecules is repulsive.

The modelling results in this study indicate a fundamental shift in term of the interaction: at low concentrations, the interaction becomes significant. This can be explained by the change in ionic bonding of Gemini surfactants as showed by neutron reflectometry[121]. At high concentrations, one of the two anions is bounded the Gemini surfactants. Whereas, at low concentrations, ~ 10% of CMC, both anions dissociate from the surfactant. Such concentration-dependent behaviour has been discussed at length in the literature [30]. Hence, at high concentrations, Gemini surfactants behave cationic surfactants: mono-charged surfactant and a counter-anion. At lower concentrations, Gemini surfactants behave differently: a double-charged surfactants surrounding by two counter-anions.

The changing charge can lead to different interactions. At low concentrations, the adsorbed surfactants interact repulsively via the counter ions. At high concentrations, the surfactant behaves as normal surfactants, i.e. being governed by Langmuir isotherm. In theory, there should be a gradual transition between the two binding states. Hence, the appropriate model should have A as a concentration-dependent parameter, instead of a constant. Such modelling would require a comprehensive development of the numerical procedure and outside the scope of this study.

5.6 Summary

In this study, the adsorption behaviour of Gemini surfactant at decane/water interface was investigated experimentally and theoretically. Consequently, a new mathematical approach was developed to fit the experiment results of equilibrium adsorption of Gemini surfactants. The new model has two adjustable parameters and and does not require Gibbs equation.

The Gemini surfactant is fundamentally different to normal cationic surfactant in previous Chapter and require new modelling equations. At equilibrium adsorption, a new model (Eq. 5-1) was developed to provide consistent fitting. The dynamic fitting obey two theoritical models, Langmuir for higher and Frumkin for lower concentrattions. The concentration-dependent behaviour can be explained by considering variable ionic bounding of the Gemini surfactant.

6 Conclusions and Recommendations

6.1 Conclusions

The study has investigated the dynamic adsorption of cationic surfactants at oil/water interface, with a new modelling framework. The new model used simple equations to relate interfacial to the bulk concentration. Consequently, the dynamic modelling was applied to obtain adsorption parameters. The dynamic model was fitted simultaneously at two different concentrations and used data at other concentrations for verifications.

The experimental and subsequent modelling were conducted for two system: surfactants: cetyl trimethyl ammonium bromide (CTAB) and Gemini surfactant (C_{14}-C_3-C_{14}) at the alkane/water interface.

In the first part of the study, two different oils were used. The results indicated a strong interaction between alkane molecules and hydrocarbon tails of surfactant at oil/water interface. From the obtained parameters, new physical insights on alkane and surfactants adsorption addition were proposed. Quantitatively, the model indicated that surfactant form a double layer at oil/water interface. The double layer was thinner as oil molecule reduced from decane to hexane. The results open new method to correctly predict the interaction between oil and surfactant molecules as well as the effects of the interactions.

In the second part, the dynamic adsorption of a Gemini surfactant, $C_{14}C_3C_{14}$ was studied. The results indicated the Gemini surfactant has very long adsorption at oil/water interface. The comprehensive modelling indicated a complicated behavior of Gemini surfactant at decane/water interface. Most significantly, the results demonstrated a variable and concentration-dependent interaction between the adsorbed molecules. Unusual behaviour of Gemini surfactant at dynamic interfacial tension requires to usage two isotherm models, Langmuir and Frumkin isotherms. At high concentrations, the Langmuir isotherm was able to predict the adsorption. Yet, Frumkin isotherm with three parameters was required for low concentrations.

6.2 Recommendation

The study has qualitatively described the influence of oil molecules on the surfactant adsorption. The proposed interactions would need further verification, especially from other methods. Unlike air/water interface, however, the oil/water interface is not readily accessible by other experimental techniques, such as neutron reflectometry or sum frequency generation. Hence, it is recommended that molecular simulation is carried out to verify the results from this study.

References

[1] S.O. Majekodunmi, O. A. Itiola, Usefulness of surface and interfacial phenomena in formulation of pharmaceutical products, International Journal of Pharmacy and Pharmaceutical Science Research, 4 (2014) 65-70.

[2] F.E. Bartell, L.O. Case, H. Brown, Interfacial Tension of Mercury in Contact with Organic Liquids, Journal of the American Chemical Society, 55 (1933) 2419-2426.

[3] C.-H. Chang, E.I. Franses, Adsorption dynamics of surfactants at the air/water interface: a critical review of mathematical models, data, and mechanisms, Colloids and Surfaces A: Physicochemical and Engineering Aspects, 100 (1995) 1-45.

[4] J. Eastoe, J.S. Dalton, Dynamic surface tension and adsorption mechanisms of surfactants at the air–water interface, Advances in Colloid and Interface Science, 85 (2000) 103-144.

[5] L.L. Schramm, E.N. Stasiuk, D.G. Marangoni, 2 Surfactants and their applications, Annual Reports Section "C" (Physical Chemistry), 99 (2003) 3-48.

[6] A.J. Prosser, E.I. Franses, Adsorption and surface tension of ionic surfactants at the air–water interface: review and evaluation of equilibrium models, Colloids and Surfaces A: Physicochemical and Engineering Aspects, 178 (2001) 1-40.

[7] N. Mucic, N.M. Kovalchuk, V. Pradines, A. Javadi, E.V. Aksenenko, J. Krägel, R. Miller, Dynamic properties of CnTAB adsorption layers at the water/oil interface, Colloids and Surfaces A: Physicochemical and Engineering Aspects, 441 (2014) 825-830.

[8] S.-Y. Lin, K. McKeigue, C. Maldarelli, Diffusion-controlled surfactant adsorption studied by pendant drop digitization, American Institute of Chemical Engineering Journal, 36 (1990) 1785-1795.

[9] E.V. Aksenenko, V.B. Fainerman, J.T. Petkov, R. Miller, Dynamic surface tension of mixed oxyethylated surfactant solutions, Colloids and Surfaces A: Physicochemical and Engineering Aspects, 365 (2010) 210-214.

[10] P. Joos, Kinetic Equations for Transfer-Controlled Adsorption Kinetics, Journal of Colloid and Interface Science, 171 (1995) 399-405.

[11] Dukhin. S.S, Kretzschmar. G, M. R, Dynamics of Adsorption at Liquid Interfaces:

Theory, Experiment, Application, Elsevier Science, 1995.
[12] A. Javadi, N. Mucic, D. Vollhardt, V.B. Fainerman, R. Miller, Effects of dodecanol on the adsorption kinetics of SDS at the water–hexane interface, Journal of Colloid and Interface Science, 351 (2010) 537-541.
[13] V. Pradines, V.B. Fainerman, E.V. Aksenenko, J. Krägel, N. Mucic, R. Miller, Adsorption of alkyl trimethylammonium bromides at the water/air and water/hexane interfaces, Colloids and Surfaces A: Physicochemical and Engineering Aspects, 371 (2010) 22-28.
[14] M. Ferrari, L. Liggieri, F. Ravera, C. Amodio, R. Miller, Adsorption Kinetics of Alkylphosphine Oxides at Water/Hexane Interface: 1. Pendant Drop Experiments, Journal of Colloid and Interface Science, 186 (1997) 40-45.
[15] N. Mucic, N.M. Kovalchuk, E.V. Aksenenko, V.B. Fainerman, R. Miller, Adsorption layer properties of alkyltrimethylammonium bromides at interfaces between water and different alkanes, Journal of Colloid and Interface Science, 410 (2013) 181-187.
[16] B.-B. Lee, P. Ravindra, E.-S. Chan, New drop weight analysis for surface tension determination of liquids, Colloids and Surfaces A: Physicochemical and Engineering Aspects, 332 (2009) 112-120.
[17] Javadi. A., Mucic. N, Karbaschi. M, Won. J. Y, Fainerman. V. B, Sharipova. A, Aksenenko. E. V, Kovalchuk. V. I, Kovalchuk. N. M, Makievski. A. V, Krägel. J, Miller. R, D. habi, Interfacial Dynamics Methods, Encyclopedia of Colloid and Interface Science, pp 637-676.
[18] N. Mucic, A. Javadi, N.M. Kovalchuk, E.V. Aksenenko, R. Miller, Dynamics of interfacial layers—Experimental feasibilities of adsorption kinetics and dilational rheology, Advances in Colloid and Interface Science, 168 (2011) 167-178.
[19] G. Grossmann, I. Larsson, R. Nilsson, B. Robertson, L. Rydhag, P. Stenius, Lung Expansion in Premature Newborn Rabbits Treated with Emulsified Synthetic Surfactant; Principles for Experimental Evaluation of Synthetic Substitutes for Pulmonary Surfactant, Respiration, 45 (1984) 327-338.
[20] J. Eastoe, R.F. Tabor, Chapter 6 - Surfactants and Nanoscience, in: D.B. Palazzo (Ed.) Colloidal Foundations of Nanoscience, Elsevier, Amsterdam, 2014, pp. 135-157.

[21] Y. He, P. Yazhgur, A. Salonen, D. Langevin, Adsorption–desorption kinetics of surfactants at liquid surfaces, Advances in Colloid and Interface Science, 222 (2015) 377-384.

[22] W.K. Kegel, G.A. Van Aken, M.N. Bouts, H.N.W. Lekkerkerker, J.T.G. Overbeek, P.L. De Bruyn, Adsorption of sodium dodecyl sulfate and cosurfactant at the planar cyclohexane-brine interface. Validity of the saturation adsorption approximation and effects of the cosurfactant chain length, Langmuir, 9 (1993) 252-256.

[23] L. Peltonen, J. Hirvonen, J. Yliruusi, The Behavior of Sorbitan Surfactants at the Water–Oil Interface: Straight-Chained Hydrocarbons from Pentane to Dodecane as an Oil Phase, Journal of Colloid and Interface Science, 240 (2001) 272-276.

[24] H.B. de Aguiar, M.L. Strader, A.G.F. de Beer, S. Roke, Surface Structure of Sodium Dodecyl Sulfate Surfactant and Oil at the Oil-in-Water Droplet Liquid/Liquid Interface: A Manifestation of a Nonequilibrium Surface State, Journal of Physical Chemistry B, 115 (2011) 2970-2978.

[25] C. Baroud, Marangoni Convection, in: D. Li (Ed.) Encyclopedia of Microfluidics and Nanofluidics, Springer US, 2014, pp. 1-8.

[26] R.J. M, K.J. T, Surfactants and Interfacial Phenomena, 4th Edition ed., John Wiley & Sons, Inc., 2012.

[27] J. Eastoe, Surfactant Aggregation and Adsorption at Interfaces, Colloid Science, Blackwell Publishing Ltd., 2009, pp. 50-76.

[28] R. Gunde, A. Kumar, S. Lehnert-Batar, R. Mäder, E.J. Windhab, Measurement of the Surface and Interfacial Tension from Maximum Volume of a Pendant Drop, Journal of Colloid and Interface Science, 244 (2001) 113-122.

[29] W. Wang, K.H. Ngan, J. Gong, P. Angeli, Observations on single drop formation from a capillary tube at low flow rates, Colloids and Surfaces A: Physicochemical and Engineering Aspects, 334 (2009) 197-202.

[30] R. Zana, Dimeric and oligomeric surfactants. Behavior at interfaces and in aqueous solution: a review, Advances in Colloid and Interface Science, 97 (2002) 205-253.

[31] I. Langmuir, Journal of the American Chemical Society, (1918).

[32] B. Von Szyskowski, Z. Journal of Physical Chemistry, (1908).

[33] A. Frumkin, Z. Journal of Physical Chemistry, (1925).

[34] E.A. Boucher, T.M. Grinchuk, A.C. Zettlemoyer, Surface activity of sodium salts of alpha-sulfo fatty esters: The air-water interface, Journal of the American Oil Chemists Society, 45 (1968) 49-52.

[35] T.D. Gurkov, T.S. Horozov, I.B. Ivanov, R.P. Borwankar, Composition of mixed adsorption layers of non-ionic surfactants an oil/water interfaces, Colloids and Surfaces A: Physicochemical and Engineering Aspects, 87 (1994) 81-92.

[36] K. Danov, P. Kralchevsky, The standard free energy of surfactant adsorption at air/water and oil/water interfaces: Theoretical vs. empirical approaches, Colloid Journal, 74 (2012) 172-185.

[37] M. Kind, W. Peukert, H. Rehage, H.P. Schuchmann, Colloid Process Engineering, Springer International Publishing, 2015.

[38] K. Mędrzycka, W. Zwierzykowski, Adsorption of Alkyltrimethylammonium Bromides at the Various Interfaces, Journal of Colloid and Interface Science, 230 (2000) 67-72.

[39] V.B. Fainerman, N. Mucic, V. Pradines, E.V. Aksenenko, R. Miller, Adsorption of Alkyltrimethylammonium Bromides at Water/Alkane Interfaces: Competitive Adsorption of Alkanes and Surfactants, Langmuir, 29 (2013) 13783-13789.

[40] V.B. Fainerman, E.V. Aksenenko, V.I. Kovalchuk, A. Javadi, R. Miller, Study of the co-adsorption of hexane from the gas phase at the surface of aqueous C10EO8 drops, Soft Matter, 7 (2011) 7860-7865.

[41] W.R. Gillap, N.D. Weiner, M. Gibaldi, Ideal behavior of sodium alkyl sulfates at various interfaces. Thermodynamics of adsorption at the oil-water interface, The Journal of Physical Chemistry, 72 (1968) 2222-2227.

[42] E. Hutchinson, Films at oil-water interfaces. I, Journal of Colloid Science, 3 (1948) 219-234.

[43] A. Salamah, C.M. Phan, H.G. Pham, Dynamic adsorption of cetyl trimethyl ammonium bromide at decane/water interface, Colloids and Surfaces A: Physicochemical and Engineering Aspects, 484 (2015) 313-317.

[44] M.L. Schlossman, A.M. Tikhonov, Molecular Ordering and Phase Behavior of Surfactants at Water-Oil Interfaces as Probed by X-Ray Surface Scattering, Annual Review of Physical Chemistry, 59 (2008) 153-177.

[45] V.B. Fainerman, E.V. Aksenenko, N. Mucic, A. Javadi, R. Miller, Thermodynamics of adsorption of ionic surfactants at water/alkane interfaces, Soft Matter, 10 (2014) 6873-6887.
[46] D. Hu, A. Mafi, K.C. Chou, Revisiting the Thermodynamics of Water Surfaces and the Effects of Surfactant Head Group, The Journal of Physical Chemistry B, (2016).
[47] Raul Zana, Jiding Xia, Gemini Surfactants: Synthesis, Interfacail and Solution - Phase Behavior, and Applications, MARCEL DEKKER, INC, 2004.
[48] F.M. Menger, C.A. Littau, Gemini surfactants: a new class of self-assembling molecules, Journal of the American Chemical Society, 115 (1993) 10083-10090.
[49] M. Borse, V. Sharma, V.K. Aswal, P.S. Goyal, S. Devi, Effect of head group polarity and spacer chain length on the aggregation properties of gemini surfactants in an aquatic environment, Journal of Colloid and Interface Science, 284 (2005) 282-288.
[50] S.D. Wettig, R.E. Verrall, Thermodynamic Studies of Aqueous m–s–m Gemini Surfactant Systems, Journal of Colloid and Interface Science, 235 (2001) 310-316.
[51] X. Wang, Q. Li, X. Chen, Z. Li, Effects of Structure Dissymmetry on Aggregation Behaviors of Quaternary Ammonium Gemini Surfactants in a Protic Ionic Liquid EAN, Langmuir, 28 (2012) 16547-16554.
[52] P. Renouf, C. Mioskowski, L. Lebeau, D. Hebrault, J.-R. Desmurs, Dimeric surfactants: First synthesis of an asymmetrical gemini compound, Tetrahedron Letters, 39 (1998) 1357-1360.
[53] R. Oda, S. J. Candau, R. Oda, I. Huc, Gemini surfactants, the effect of hydrophobic chain length and dissymmetry, Chemical Communications, (1997) 2105-2106.
[54] M.J. Rosen, T. Gao, Y. Nakatsuji, A. Masuyama, Synergism in binary mixtures of surfactants 12. Mixtures containing surfactants with two hydrophilic and two or three hydrophobic groups, Colloids and Surfaces A: Physiochemical and Engineering Aspects, 88 (1994) 1-11.
[55] R. Zana, H. Levy, D. Papoutsi, G. Beinert, Micellization of Two Triquaternary Ammonium Surfactants in Aqueous Solution, Langmuir, 11 (1995) 3694-3698.

[56] T.A. Camesano, R. Nagarajan, Micelle formation and CMC of gemini surfactants: a thermodynamic model, Colloids and Surfaces A: Physiochemical and Engineering Aspects, 167 (2000) 165-177.

[57] M. Frindi, B. Michels, H. Levy, R. Zana, Alkanediyl-.alpha.,.omega.-bis(dimethylalkylammonium bromide) Surfactants. 4. Ultrasonic Absorption Studies of Amphiphile Exchange between Micelles and Bulk Phase in Aqueous Micellar Solution, Langmuir, 10 (1994) 1140-1145.

[58] D.P. Acharya, J.M. Gutiérrez, K. Aramaki, K.-i. Aratani, H. Kunieda, Interfacial properties and foam stability effect of novel gemini-type surfactants in aqueous solutions, Journal of Colloid and Interface Science, 291 (2005) 236-243.

[59] K.M. Layn, P.G. Debenedetti, R.K. Prud'homme, A theoretical study of Gemini surfactant phase behavior, The Journal of Chemical Physics, 109 (1998) 5651-5658.

[60] R. Zana, Gemini (dimeric) surfactants, Current Opinion in Colloid & Interface Science, 1 (1996) 566-571.

[61] M.J.L. Castro, J. Kovensky, A. Fernández Cirelli, New Family of Nonionic Gemini Surfactants. Determination and Analysis of Interfacial Properties, Langmuir, 18 (2002) 2477-2482.

[62] M.S. Borse, S. Devi, Importance of head group polarity in controlling aggregation properties of cationic gemini surfactants, Advances in Colloid and Interface Science, 123–126 (2006) 387-399.

[63] N. Kumar, R. Tyagi, Industrial Applications of Dimeric Surfactants: A Review, Journal of Dispersion Science and Technology, 35 (2013) 205-214.

[64] A.J. Kirby, P. Camilleri, J.B.F.N. Engberts, M.C. Feiters, R.J.M. Nolte, O. Söderman, M. Bergsma, P.C. Bell, M.L. Fielden, C.L. García Rodríguez, P. Guédat, A. Kremer, C. McGregor, C. Perrin, G. Ronsin, M.C.P. van Eijk, Gemini Surfactants: New Synthetic Vectors for Gene Transfection, Angewandte Chemie Internatioonal Edition, 42 (2003) 1448-1457.

[65] M. El Achouri, S. Kertit, H.M. Gouttaya, B. Nciri, Y. Bensouda, L. Perez, M.R. Infante, K. Elkacemi, Corrosion inhibition of iron in 1 M HCl by some gemini surfactants in the series of alkanediyl-α,ω-bis-(dimethyl tetradecyl ammonium bromide), Progress in Organic Coatings, 43 (2001) 267-273.

[66] M.J. Rosen, X.Y. Hua, Dynamic surface tension of aqueous surfactant solutions: 2. Parameters at 1 s and at mesoequilibrium, Journal of Colloid and Interface Science, 139 (1990) 397-407.

[67] I.B. Ivanov, K.P. Ananthapadmanabhan, A. Lips, Adsorption and structure of the adsorbed layer of ionic surfactants, Advances in Colloid and Interface Science, 123–126 (2006) 189-212.

[68] T. Gao, M.J. Rosen, Dynamic Surface Tension of Aqueous Surfactant Solutions: 7. Physical Significance of Dynamic Parameters and the Induction Period, Journal of Colloid and Interface Science, 172 (1995) 242-248.

[69] R. Jiang, J. Zhao, Y. Ma, Dynamic adsorption of opposite-charged Gemini surfactant mixture at air/water interface, Colloids and Surfaces A: Physiochemical and Engineering Aspects, 289 (2006) 233-236.

[70] T. Gao, M. Rosen, Dynamic surface tension of aqueous surfactant solutions. 6. Compounds containing two hydrophilic head groups and two or three hydrophobic groups and their mixtures with other surfactants, Journal of the American Oil Chemists Society, 71 (1994) 771-776.

[71] V. Seredyuk, E. Alami, M. Nydén, K. Holmberg, A.V. Peresypkin, F.M. Menger, Adsorption of zwitterionic gemini surfactants at the air–water and solid–water interfaces, Colloids and Surfaces A: Physiochemical and Engineering Aspects, 203 (2002) 245-258.

[72] Z.X. Li, C.C. Dong, J.B. Wang, R.K. Thomas, J. Penfold, Unusual Surface Structure in Layers of Cationic Gemini Surfactants Adsorbed at the Air/Water Interface: A Neutron Reflection Study, Langmuir, 18 (2002) 6614-6622.

[73] R. Jiang, Y.-H. Ma, J.-X. Zhao, Adsorption dynamics of binary mixture of Gemini surfactant and opposite-charged conventional surfactant in aqueous solution, Journal of Colloid and Interface Science, 297 (2006) 412-418.

[74] X. Du, H. Wu, Y. Lu, Study on the Interfacial Tensions Between Oils and Alkylbenzene Sulfonate Gemini Surfactant Solutions, Journal of Dispersion Science and Technology, 30 (2009) 61-64.

[75] L. Han, Z. Ye, H. Chen, P. Luo, The interfacial tension between cationic gemini surfactant solution and crude oil, Journal of surfactants and detergents, 12 (2009) 185-190.

[76] H. Chen, L. Han, P. Luo, Z. Ye, The interfacial tension between oil and gemini surfactant solution, Surface Science, 552 (2004) L53-L57.

[77] Q. Zhang, Q. Zhao, D.-Z. Sun, X.-L. Wei, J. Liu, Dynamic Interfacial Tension of a Gemini Surfactant: N,N′-Didodecyl-2-Hydroxyl-N,N,N′,N′-Tetramethyl-Dichloride at n-Decane/Water Interface, Journal of Dispersion Science Technology, 30 (2009) 340-345.

[78] H. Xi Yuan, M.J. Rosen, Dynamic surface tension of aqueous surfactant solutions: I. Basic paremeters, Journal of Colloid and Interface Science, 124 (1988) 652-659.

[79] X.Y. Hua, M.J. Rosen, Dynamic surface tension of aqueous surfactant solutions: 3. Some effects of molecular structure and environment, Journal of Colloid and Interface Science, 141 (1991) 180-190.

[80] M. Rosen, X. Hua, Z. Zhu, Dynamic Surface Tension of Aqueous Surfactant Solutions: IV Relationship to Foaming, in: K.L. Mittal, D.O. Shah (Eds.) Surfactants in Solution, Springer US, 1991, pp. 315-327.

[81] M.J. Rosen, T. Gao, Dynamic Surface Tension of Aqueous Surfactant Solutions: 5. Mixtures of Different Charge Type Surfactants, Journal of Colloid and Interface Science, 173 (1995) 42-48.

[82] M.J. Rosen, L.D. Song, Dynamic Surface Tension of Aqueous Surfactant Solutions 8. Effect of Spacer on Dynamic Properties of Gemini Surfactant Solutions, Journal of Colloid and Interface Science, 179 (1996) 261-268.

[83] K.J. Beers, Numerical methods for chemical engineering: applications in Matlab., Cambridge University Press, 2007.

[84] KAWALE. D, Influence of dynamic surface tension on foams: application in gas well deliquification, in, Delft University of Technology, 2012.

[85] C.M. Phan, T.N. Le, S.-i. Yusa, A new and consistent model for dynamic adsorption of CTAB at air/water interface, Colloids and Surfaces A: Physicochemical and Engineering Aspects, 406 (2012) 24-30.

[86] D.C. England, J.C. Berg, Transfer of surface-active agents across a liquid-liquid interface, American Institute of Chemical Engineers Journal, 17 (1971) 313-322.

[87] L. Junji, W. Chuangye, M. Ulf, Diffusion-controlled Adsorption Kinetics at Air/Solution Surface Studied by Maximum Bubble Pressure Method, Chinese Journal of Chemical Engineering, 12 (2004) 577-581.

[88] A.F.H. Ward, L. Tordai, Time-Dependence of Boundary Tensions of Solutions I. The Role of Diffusion in Time-Effects, The Journal of Chemical Physics, 14 (1946) 453-461.

[89] X. Li, R. Shaw, G.M. Evans, P. Stevenson, A simple numerical solution to the Ward–Tordai equation for the adsorption of non-ionic surfactants, Computers & Chemical Engineering, 34 (2010) 146-153.

[90] R. Van den Bogaert, P. Joos, Dynamic surface tensions of sodium myristate solutions, The Journal of Physical Chemistry, 83 (1979) 2244-2248.

[91] E. Rillaerts, P. Joos, Measurement of the dynamic surface tension and surface dilational viscosity of adsorbed mixed monolayers, Journal of Colloid and Interface Science, 88 (1982) 1-7.

[92] V.B. Fainerman, A.V. Makievski, R. Miller, The analysis of dynamic surface tension of sodium alkyl sulphate solutions, based on asymptotic equations of adsorption kinetic theory, Colloids and Surfaces A: Physicochemical and Engineering Aspects, 87 (1994) 61-75.

[93] C.M. Phan, A.V. Nguyen, G.M. Evans, Dynamic adsorption of sodium dodecylbenzene sulphonate and dowfroth 250 onto the air–water interface, Minerals Engineering, 18 (2005) 599-603.

[94] H.J.V. Tyrrell, k.R. Harris, Diffusion in Liquids: A Theoretical and Experimental Study in, Butterworth & Co 1984.

[95] C. Tropea, A.L. Yarin, J.F. Foss, Springer Handbook of Experimental Fluid Mechanics, Springer Berlin Heidelberg, 2007.

[96] A. Arnott, D.A. Ress, E.R. Morris, Molecular Biophysics of the Extracellular Matrix. Humana Press, 1984.

[97] D.G. Leaist, L. Hao, Simultaneous Measurement of Mutual Diffusion and Intradiffusion by Taylor Dispersion, The Journal of Physical Chemistry, 98 (1994) 4702-4706.

[98] G. D'Errico, O. Ortona, L. Paduano, V. Vitagliano, Transport Properties of Aqueous Solutions of Alkyltrimethylammonium Bromide Surfactants at 25°C, Journal of Colloid and Interface Science, 239 (2001) 264-271.

[99] M. Abe, J.F. Scamehorn, Mixed Surfactant Systems, CRC Press, 2004.

[100] C.M. Phan, T.N. Le, C.V. Nguyen, S.-i. Yusa, Modeling Adsorption of Cationic Surfactants at Air/Water Interface without Using the Gibbs Equation, Langmuir, 29 (2013) 4743-4749.

[101] C.V. Nguyen, T.V. Nguyen, C.M. Phan, Dynamic adsorption of a gemini surfactant at the air/water interface, Colloids and Surfaces A: Physicochemical and Engineering Aspects, 482 (2015) 365-370.

[102] T.F. Tadros, Emulsion formation and stability, John Wiley & Sons, 2013.

[103] M.L. Schlossman, X-ray scattering from liquid–liquid interfaces, Physica B: Condensed Matter, 357 (2005) 98-105.

[104] Z.X. Li, J.R. Lu, G. Fragneto, R.K. Thomas, B.P. Binks, P.D.I. Fletcher, J. Penfold, Neutron reflectivity studies of Aerosol-OT monolayers adsorbed at the oil/water, air/water and hydrophobic solid/wate interfaces, Colloids and Surfaces A: Physicochemical and Engineering Aspects, 135 (1998) 277-281.

[105] M.L. Schlossman, Liquid–liquid interfaces: studied by X-ray and neutron scattering, Current Opinion in Colloid & Interface Science, 7 (2002) 235-243.

[106] J.R. Lu, Z.X. Li, R.K. Thomas, B.P. Binks, D. Crichton, P.D.I. Fletcher, J.R. McNab, J. Penfold, The Structure of Monododecyl Pentaethylene Glycol Monolayers with and without Added Dodecane at the Air/Solution Interface: A Neutron Reflection Study, The Journal of Physical Chemistry B, 102 (1998) 5785-5793.

[107] X. Wang, S.Y. Lee, K. Miller, R. Welbourn, I. Stocker, S. Clarke, M. Casford, P. Gutfreund, M.W.A. Skoda, Cation Bridging Studied by Specular Neutron Reflection, Langmuir, 29 (2013) 5520-5527.

[108] Dixon. J. K, Weith. A. J, Argyle. A. A, S.D. J, Measurement of the Adsorption of Surface-Active Agent at a Solution – Air Interface by a Radiotracer Method, Nature, 168 (1949) 845.

[109] Matuura. R, Kimizuka. H, Miyamoto. S, S. R, The Study of the Adsorption of Detergents at a Solution-Air Interface by Radiotracer Method. I. Adsorption Isotherm for the Solution of Sodium Alkyl Sulfates, BULLETIN OF THE CHEMICAL SOCIETY OF JAPAN, 31 (1958) 532-538.

[110] D.J. Salley, A.J. Weith, A.A. Argyle, J.K. Dixon, Measurement of the Adsorption of Surface-Active Agents at a Solution/Air Interface by a Radiotracer Method, Proceedings of the Royal Society of London A: Mathematical, Physical and Engineering Sciences, 203 (1950) 42-55.

[111] G.R. Burnett, R. Atkin, S. Hicks, J. Eastoe, Surfactant-Free “Emulsions” Generated by Freeze−Thaw, Langmuir, 20 (2004) 5673-5678.

[112] M.G. Steinmetz, C. Yu, Far-UV photochemistry of 1,1-dimethyl-1-silacyclopent-3-ene: photoextrusion of dimethylsilylene and stereoselective 1,4-addition of methanol to an intermediate vinylsilirane, Organometallics, 11 (1992) 2686-2690.

[113] J.M. Andreas, E.A. Hauser, W.B. Tucker, BOUNDARY TENSION BY PENDANT DROPS1, The Journal of Physical Chemistry, 42 (1937) 1001-1019.

[114] H.Y. Jennings, Apparatus for Measuring Very Low Interfacial Tensions, Review of Scientific Instruments, 28 (1957) 774-777.

[115] Y.Y. Zuo, C. Do, A.W. Neumann, Automatic measurement of surface tension from noisy images using a component labeling method, Colloids and Surfaces A: Physiochemical and Engineering Aspects, 299 (2007) 109-116.

[116] J. Jůza, The pendant drop method of surface tension measurement: equation interpolating the shape factor tables for several selected planes, Czechoslovak Journal of Physics, 47 (1997) 351-357.

[117] A.Y. Dandekar, Petroleum Reservoir Rock and Fluid Properties, CRC Press, 2013.

[118] T. Ferreira, W. Rasband, ImageJ User Guide. IJ1. 46r, (2012).

[119] R.M. Prokop, A. Jyoti, M. Eslamian, A. Garg, M. Mihaila, O.I. del Río, S.S. Susnar, Z. Policova, A.W. Neumann, A study of captive bubbles with axisymmetric drop shape analysis, Colloids and Surfaces A: Physicochemical and Engineering Aspects, 131 (1998) 231-247.

[120] T. Gilányi, I. Varga, C. Stubenrauch, R. Mészáros, Adsorption of alkyl trimethylammonium bromides at the air/water interface, Journal of Colloid and Interface Science, 317 (2008) 395-401.

[121] Z.X. Li, C.C. Dong, R.K. Thomas, Neutron Reflectivity Studies of the Surface Excess of Gemini Surfactants at the Air−Water Interface, Langmuir, 15 (1999) 4392-4396.

[122] T.W. Davey, W.A. Ducker, A.R. Hayman, J. Simpson, Krafft Temperature Depression in Quaternary Ammonium Bromide Surfactants, Langmuir, 14 (1998) 3210-3213.

[123] D. Guilfoyle, G. Kaur, J. Hrabe, Principles and limitations of NMR diffusion measurements, 2007.

[124] S.J. Gibbs, C.S. Johnson Jr, A PFG NMR experiment for accurate diffusion and flow studies in the presence of eddy currents, Journal of Magnetic Resonance, (1969), 93 (1991) 395-402.

[125] V.V. Krishnan, K.H. Thornton, M. Cosman, An improved experimental scheme to measure self-diffusion coefficients of biomolecules with an advantageous use of radiation damping, Chemical Physics Letters, 302 (1999) 317-323.

[126] E.O. Stejskal, J.E. Tanner, Spin Diffusion Measurements: Spin Echoes in the Presence of a Time-Dependent Field Gradient, The Journal of Chemical Physics, 42 (1965) 288-292.

[127] P. Cheng, D. Li, L. Boruvka, Y. Rotenberg, A.W. Neumann, Automation of axisymmetric drop shape analysis for measurements of interfacial tensions and contact angles, Colloids and Surfaces, 43 (1990) 151-167.

[128] L. Liggieri, M. Ferrari, A. Massa, F. Ravera, Molecular reorientation in the adsorption of some CiEj at the water-air interface, Colloids and Surfaces A: Physiochemical and Engineering Aspects, 156 (1999) 455-463.

[129] R. Miller, E.V. Aksenenko, L. Liggieri, F. Ravera, M. Ferrari, V.B. Fainerman, Effect of the Reorientation of Oxyethylated Alcohol Molecules within the Surface Layer on Equilibrium and Dynamic Surface Pressure, Langmuir, 15 (1999) 1328-1336.

[130] E.C. Donaldson, G.V. Chilingarian, T.F. Yen, Enhanced oil recovery, II: Processes and operations, Elsevier, 1989.

[131] L.S. Romsted, Surfactant Science and Technology: Retrospects and Prospects, CRC Press, 2014.

Appendix 1

1- CTAB/Decane interface

Equilibrium Calculations

a. Fitting equilibrium results by new model

				0.02281		0.35232
Concentratio(mM)	*Experiments(mN/m)*	***Eq. (2-7)***	*Equi G (Ge/Gm)*	0.00393	Eq. (2-32)	0.62063
0.00E+00	52.28	52.28		0	52.28	0
2.00E-04	35.22	***3.52E+01***	*0.465576172*	2.2E-06	3.59E+01	0.42975
4.00E-04	24.81	***2.48E+01***	*0.635253906*	2.8E-05	24.61301	0.0388
6.00E-04	17.26	***1.73E+01***	*0.723144531*	0.00205	16.88805	0.13984
8.00E-04	11.477	***1.14E+01***	*0.776855469*	0.00184	11.58761	0.01224

b. Applying Szyszkowski equation where multiple solutions were obtained

Case 1

KF (mol-1)	3770.444	
Gm (mol/m^2)	1.19E-05	
A	0	
Concentratio(mM)	***Case 3***	*Equi G (Ge/Gm)*
0.00E+00	52.28	
2.50E-07	***5.23E+01***	*0.000941753*
5.00E-07	***5.22E+01***	*0.001881599*
1.00E-06	***5.22E+01***	*0.003755569*
2.00E-05	***5.01E+01***	*0.070129395*
0.00005	***4.72E+01***	*0.158569336*
0.0001	***4.28E+01***	*0.273681641*
2.00E-04	***3.57E+01***	*0.429931641*
4.00E-04	***2.51E+01***	*0.601074219*
6.00E-04	***1.73E+01***	*0.693847656*
8.00E-04	***1.11E+01***	*0.751464844*

Case 2

KF (mol-1)	4500	
Gm (mol/m^2)	1.08E-05	
A	0	
Concentration	***Case 2***	*Equi G (Ge/Gm)*
0.00E+00	52.28	
2.50E-07	***5.22E+01***	*0.001124382*
5.00E-07	***5.22E+01***	*0.002244949*
1.00E-06	***5.22E+01***	*0.004482269*
2.00E-05	***5.00E+01***	*0.082580566*
0.00005	***4.69E+01***	*0.18371582*
0.0001	***4.24E+01***	*0.310302734*
2.00E-04	***3.51E+01***	*0.473876953*
4.00E-04	***2.48E+01***	*0.643066406*
6.00E-04	***1.73E+01***	*0.729980469*
8.00E-04	***1.15E+01***	*0.782714844*

Case 3

KF (mol-1)	2300	
Gm (mol/m^2)	1.63E-05	
A	0	
Concentratio(mM)	**Case 1**	Equi G (Ge/Gm)
0.00E+00	52.28	
2.50E-07	**5.23E+01**	0.000574589
5.00E-07	**5.22E+01**	0.001149178
1.00E-06	**5.22E+01**	0.00229454
2.00E-05	**5.05E+01**	0.04397583
0.00005	**4.79E+01**	0.103088379
0.0001	**4.39E+01**	0.186889648
2.00E-04	**3.70E+01**	0.315185547
4.00E-04	**2.59E+01**	0.479248047
6.00E-04	**1.73E+01**	0.579589844
8.00E-04	**1.01E+01**	0.647949219

Case 4

KF (mol-1)	4354.871	
Gm (mol/m^2)	1.1E-05	
A	0	
Concentratio(mM)	**Case 4**	Equi G (Ge/Gm)
0.00E+00	52.28	
2.50E-07	**5.23E+01**	0.001088142
5.00E-07	**5.22E+01**	0.00217247
1.00E-06	**5.22E+01**	0.004337311
2.00E-05	**5.00E+01**	0.08013916
0.00005	**4.69E+01**	0.178833008
0.0001	**4.24E+01**	0.303466797
2.00E-04	**3.52E+01**	0.465576172
4.00E-04	**2.48E+01**	0.635253906
6.00E-04	**1.73E+01**	0.723144531
8.00E-04	**1.14E+01**	0.776855469

2- CTAB/Hexane interface

a. New model fittings

			0.5864032		49.5	
concentration (M)	Expriments(mN/m)	Eq. (2-7)	1.3754747	EquG	Equation (2-32)	1.01375233
0.00E+00	49.5	49.5	0		4.95E+01	0
3.00E-04	21.62283574	2.25E+01	0.7940926	0.63916	2.25E+01	0.73305345
4.00E-04	17.28387169	1.74E+01	0.0116208	0.702637	17.27831795	3.0844E-05
5.00E-04	13.81062058	1.31E+01	0.5697613	0.747559	13.28083947	0.28066803

b. Szyszkowski equation

Case 1

KF (mol-1)	7111	
Gm (mol/m^2)	9.70E-06	
A	0	
Concentratio(M)	Case 2	Equi G (Ge/Gm)
0.00E+00	49.50	
2.50E-07	4.95E+01	0.001774788
5.00E-07	4.94E+01	0.003541946
1.00E-06	4.93E+01	0.007061005
2.00E-05	4.63E+01	0.124633789
0.00005	4.22E+01	0.262451172
0.0001	3.66E+01	0.415771484
3.00E-04	2.20E+01	0.681152344
4.00E-04	1.71E+01	0.739746094
5.00E-04	1.30E+01	0.780761719
6.00E-04	9.56E+00	0.810058594

Case 2

KF (mol-1)	5909	
Gm (mol/m^2)	1.07E-05	
A	0	
Concentratio(M)	Case 1	Equi G (Ge/Gm)
0.00E+00	49.50	
2.50E-07	4.95E+01	0.001475334
5.00E-07	4.94E+01	0.002946854
1.00E-06	4.93E+01	0.005870819
2.00E-05	4.65E+01	0.105651855
0.00005	4.26E+01	0.228149414
0.0001	3.72E+01	0.371337891
3.00E-04	2.25E+01	0.639160156
4.00E-04	1.74E+01	0.702636719
5.00E-04	1.31E+01	0.747558594
6.00E-04	9.44E+00	0.779785156

Case 3

KF (mol-1)	9909	
Gm (mol/m^2)	8.10E-06	
A	0	
Concentratio(M)	Case 3	Equi G (Ge/Gm)
0.00E+00	49.50	
2.50E-07	4.95E+01	0.002470016
5.00E-07	4.94E+01	0.004932404
1.00E-06	4.93E+01	0.009819031
2.00E-05	4.59E+01	0.165405273
0.00005	4.14E+01	0.331298828
0.0001	3.57E+01	0.497558594
3.00E-04	2.18E+01	0.748535156
4.00E-04	1.74E+01	0.798339844
5.00E-04	1.36E+01	0.832519531
6.00E-04	1.06E+01	0.855957031

Case 4

KF (mol-1)	6222	
Gm (mol/m^2)	1.04E-05	
A	0	
Concentratio(M)	Case 4	Equi G (Ge/Gm)
0.00E+00	49.50	
2.50E-07	4.95E+01	0.001553535
5.00E-07	4.94E+01	0.003103256
1.00E-06	4.93E+01	0.006183624
2.00E-05	4.65E+01	0.110656738
0.00005	4.25E+01	0.237182617
0.0001	3.71E+01	0.383544922
3.00E-04	2.24E+01	0.650878906
4.00E-04	1.73E+01	0.713378906
5.00E-04	1.32E+01	0.756347656
6.00E-04	9.51E+00	0.788574219

Appendix 2

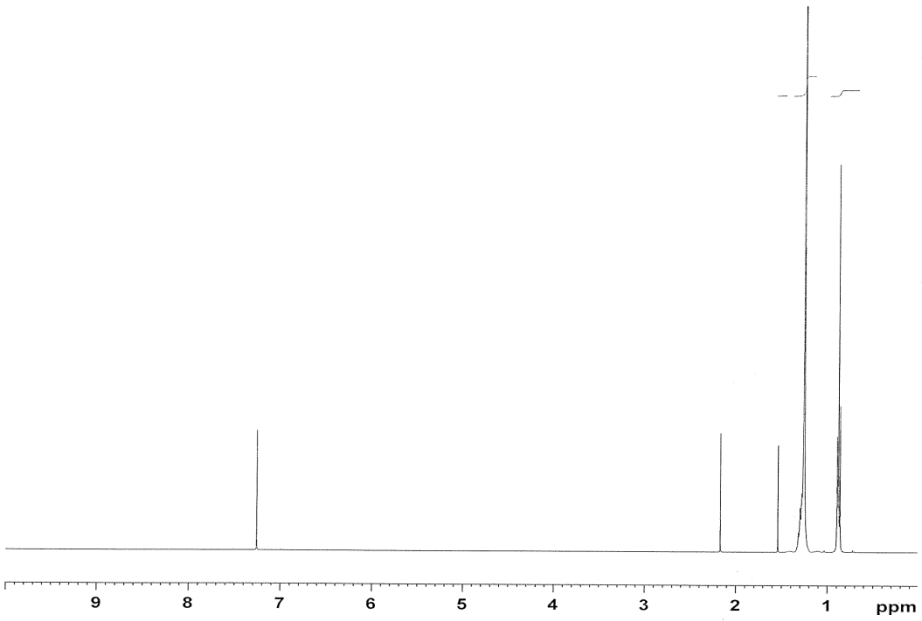

Figure A-1: NMR image for hexane as received (withpout purification)

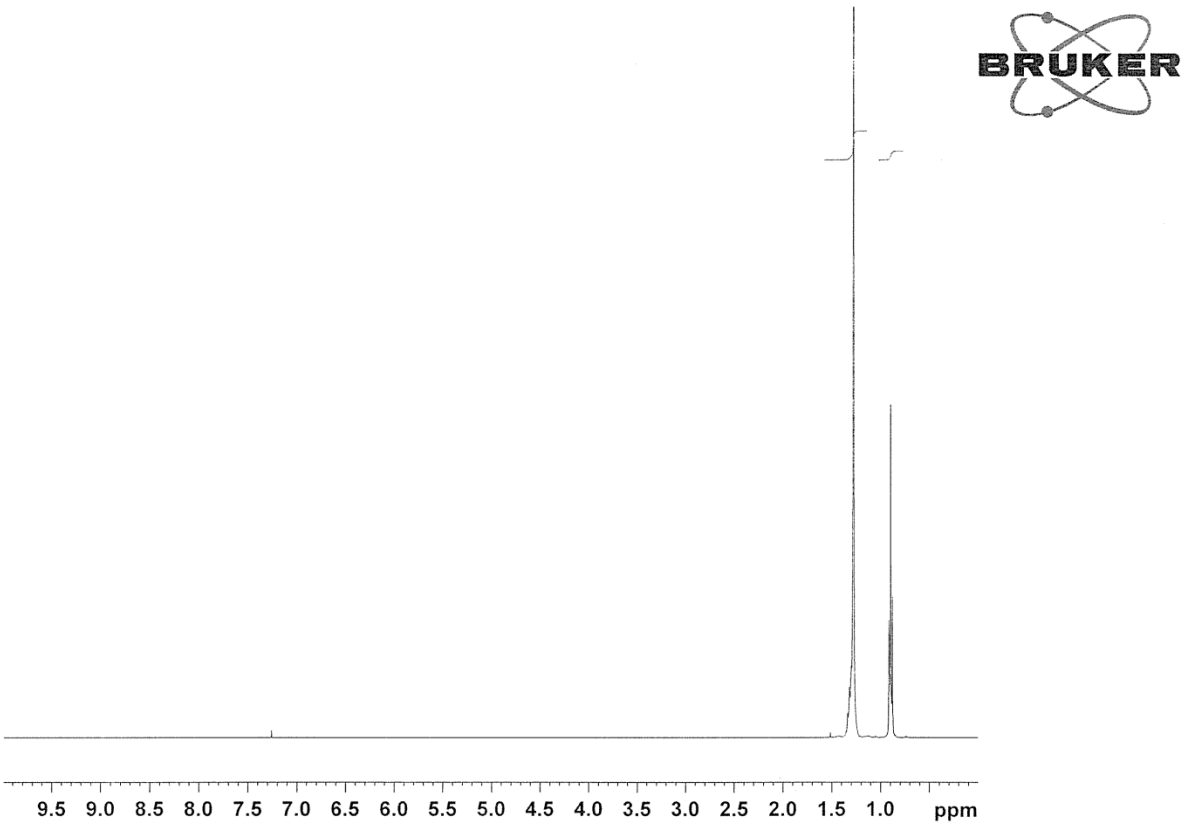

Figure A-2: NMR image for hexane after purification.

Appendix 3

Numerical procedure to calculate diffusion:

```
Function Diffusion2(tp, Cb, KF, a, D, td, nd, l, delt)
'This function calculate the dimensionless surface conc at tp given bulk conc cb
'tp,t0 in ms, c in mol
Dim n, dt, A1, A2, Cs1, Cs2, Cs3, G1, G2, G3, Err, Pi, i, ii
Dim dtt, temp(14100, 1)
Dim T(14000), G(14000), Cs(14000), F1, F2, F3

'============================================== calculated time step
For i = 1 To nd
T(i) = tt(i, nd, td, l)
Next i

'============================== timestep after td
n = nd + Int((tp - td) / delt)
dtt = (tp - td) / (n - nd)
For i = nd + 1 To n
T(i) = td + (i - nd) * dtt
Next i

'==================================
G(0) = 0: T(0) = 0: Cs(0) = 0: temp(0, 0) = 0
Pi = Atn(1) * 4: A1 = (D / Pi) ^ (0.5)
For i = 1 To n
A2 = 2 * Cb * A1 * (T(i) ^ 0.5) - A1 * Cs(i - 1) * (T(i) - T(i - 1)) ^ (0.5)
For ii = 1 To i – 1
A2 = A2 + A1 * (Cs(ii) + Cs(ii - 1)) * ((T(i) - T(ii)) ^ (0.5) - (T(i) - T(ii - 1)) ^ (0.5))
Next ii 'calculate A2
Err = 1: Cs1 = Cb: Cs2 = 0 'Cs(i - 1): 'limits of Cs(i)
```

```
'====================================== bisection
While Err > (0.00001) 'And test(i) < 29
G1 = GFr(A1, A2, Cs1, T(i), T(i - 1)): F1 = F(Cs1, KF, G1, a)
G2 = GFr(A1, A2, Cs2, T(i), T(i - 1)): F2 = F(Cs2, KF, G2, a)
If F1 * F2 < 0 Then
Cs3 = (Cs2 + Cs1) / 2 'Cs2 + Abs((Cs1 - Cs2) * F2 / (Abs(F2) + Abs(F1))) 'dividing
point
G3 = GFr(A1, A2, Cs3, T(i), T(i - 1)): F3 = F(Cs3, KF, G3, a)
If F3 = 0 Then
Err = 0
Else
If F3 * F2 < 0 Then
Cs1 = Cs3: Err = Abs(Cs1 - Cs2) / Cs1
Else
Cs2 = Cs3: Err = Abs(Cs1 - Cs2) / Cs1
End If
End If
G(i) = G3: Cs(i) = Cs3
'Debug.Print i
Else
Diffusion2 = "fail": GoTo 100
End If
Wend

'======================================end bisection
temp(i, 0) = G(i): temp(i, 1) = Cs(i)
Next i

'==================================
Diffusion2 = temp
100
End Function
Function tt(i, nd, td, l)
```

```
If i > nd Then
tt = td + (i - nd) * td * (Exp(l) - Exp((nd - 1) * l / nd)) / (Exp(l) - 1)
Else
tt = td * (Exp(i * l / nd) - 1) / (Exp(l) - 1)
End If
End Function
Function F(Cs, KF, G, a)
'calculate function F from F isotherm
F = Cs * (1 - G) - (1 / KF) * G * Exp(-a * G)
End Function
Function GFr(A1, A2, Cs, t2, t1)
'cal surface conc using diffusion sol
GFr = A2 - A1 * Cs * ((t2 - t1) ^ 0.5)
End Function
Function EquG(Cb, KF, a)
'calculate function F from F isotherm
Dim G1, G2, G3, Err, F1, F2, F3
Err = 1: G1 = 0: G2 = 1
While Err > (0.001)
F1 = F(Cb, KF, G1, a): F2 = F(Cb, KF, G2, a)
If F1 * F2 < 0 Then
G3 = (G2 + G1) / 2: F3 = F(Cb, KF, G3, a)
 If F3 = 0 Then
 Err = 0
Else
If F3 * F2 < 0 Then
G1 = G3: Err = Abs(G1 - G2) / G2
Else
G2 = G3: Err = Abs(G1 - G2) / G2
End If
    End If
EquG = G3
'Debug.Print i
```

```
Else
EquG = "fail": GoTo 100
End If
Wend
100
End Function
```